U.S. DEPARTMENT OF COMMERCE
National Technical Information Service

AD-A028 882

Compressor Critical Response Time Determination Study

Pratt and Whitney Aircraft

June 30, 1976

244139

AFAPL-TR-76-45

COMPRESSOR CRITICAL RESPONSE TIME DETERMINATION STUDY

PRATT & WHITNEY AIRCRAFT
DIVISION OF UNITED TECHNOLOGIES CORPORATION
EAST HARTFORD, CONNECTICUT 06108

30 JUNE 1976

TECHNICAL REPORT AFAPL-TR-76-45
FINAL REPORT FOR PERIOD 15 JUNE 1975 – 15 APRIL 1976

Approved for public release; distribution unlimited

AIR FORCE AERO-PROPULSION LABORATORY
AIR FORCE WRIGHT AERONAUTICAL LABORATORIES
AIR FORCE SYSTEMS COMMAND
WRIGHT-PATTERSON AIR FORCE BASE, OHIO 45433

NOTICE

When Government drawings, specifications, or other data are used for any purpose other than in connection with a definitely related Government procurement operation, the United States Government thereby incurs no responsibility nor any obligation whatsoever; and the fact that the government may have formulated, furnished, or in any way supplied the said drawings, specifications, or other data, is not to be regarded by implication or otherwise as in any manner licensing the holder or any other person or corporation, or conveying any rights or permission to manufacture, use, or sell any patented invention that may in any way be related thereto.

This is the final Technical Report proposed by Pratt & Whitney Aircraft Division of United Technologies Corporation. The effort was sponsored by the Air Force Aero Propulsion Laboratory, Air Force Systems Command, Wright-Patterson AFB, Ohio under Contract Nr F33615-75-C-2036 for the period 15 June 1975 – 15 April 1976. The work herein was accomplished under Project Nr 3066, with Mr. John E. Lueke, AFAPL/TBA, as Project Engineer. Mr. R. S. Mazzawy of Pratt & Whitney Aircraft was technically responsible for the work. Other Pratt & Whitney Aircraft personnel who contributed to the program were Messrs. G. A. Banks, C. R. Weber, and D. E. Haddad.

This report has been reviewed by the Information Office, (ASD/OIP) and is releasable to the National Technical Information Service (NTIS). At NTIS, it will be available to the general public, including foreign nations.

This technical report has been reviewed and is approved for publication.

John E. Lueke

JOHN E. LUEKE, GS-11
Project Engineer

FOR THE COMMANDER

George H. Seely

GEORGE H. SEELY, TAM
Simulation Techniques
Performance Branch

Copies of this report should not be returned unless return is required by security considerations, contractual obligations, or notice on a specific document.

AIR FORCE - 20 AUGUST 76 - 150

UNCLASSIFIED

SECURITY CLASSIFICATION OF THIS PAGE (When Data Entered)

REPORT DOCUMENTATION PAGE

READ INSTRUCTIONS BEFORE COMPLETING FORM

1. REPORT NUMBER AFAPL-TR-76-45	2. GOVT ACCESSION NO.	3. RECIPIENT'S CATALOG NUMBER
4. TITLE (and Subtitle) COMPRESSOR CRITICAL RESPONSE TIME DETERMINATION STUDY Final Report		5. TYPE OF REPORT & PERIOD COVERED Final Report 15 June 1975 15 April 1976 6. PERFORMING ORG. REPORT NUMBER PWA - 5415
7. AUTHOR(s) R. S. Mazzawy, G. A. Banks, and C. R. Weber		8. CONTRACT OR GRANT NUMBER(s) F33615-75-C-2036
9. PERFORMING ORGANIZATION NAME AND ADDRESS Pratt & Whitney Aircraft Division of United Technologies Corporation East Hartford, Connecticut 06108		10. PROGRAM ELEMENT, PROJECT, TASK AREA & WORK UNIT NUMBERS Proj. No. 3066
11. CONTROLLING OFFICE NAME AND ADDRESS Air Force Aero Propulsion Laboratory (TBA) Wright-Patterson AFB, Ohio 45433		12. REPORT DATE 30 June 1976 13. NUMBER OF PAGES 57
14. MONITORING AGENCY NAME & ADDRESS(if different from Controlling Office) NPRO - United Technologies Corporation Pratt & Whitney Aircraft East Hartford, Connecticut 06108		15. SECURITY CLASS (of this report) UNCLASSIFIED 15a. DECLASSIFICATION DOWNGRADING SCHEDULE

16. DISTRIBUTION STATEMENT (of this Report)

Approved for public release; Distribution Unlimited

17. DISTRIBUTION STATEMENT (of the abstract entered in Block 20, if different from Report)

18. SUPPLEMENTARY NOTES

19. KEY WORDS (Continue on reverse side if necessary and identify by block number)

Compressor Stall
Inlet Flow Distortion
Compressor Modeling
Compressor Stability

20. ABSTRACT (Continue on reverse side if necessary and identify by block number)

Critical response time may be defined as the time period or duration of a compressor inlet flow distortion required for a significant effect on compressor stability. The knowledge of this time period is important as a basis for evaluating time variant inlet distortion data for its potential impact on compressor stall margin. This period can be related to the time required for fluid to travel the length of a compressor by defining a reduced frequency parameter.

(Reduced Frequency = π · Distortion Frequency · Compressor Length/Fluid Velocity)

DD FORM 1 JAN 73 1473 EDITION OF 1 NOV 65 IS OBSOLETE

UNCLASSIFIED

SECURITY CLASSIFICATION OF THIS PAGE (When Data Entered)

Critical response time $\frac{1}{\text{Distortion Frequency}}$ can be defined for any compressor, once the critical value of reduced frequency in ascertained. Results of a mathematical model of a compressor system demonstrate that the critical value of reduced frequency is between 1.0 and 5.0. An inspection of available data indicates that a value of approximately 2.0 is the critical value.

TABLE OF CONTENTS

LIST OF SYMBOLS

L	Length
F	Frequency
R.F.	Reduced Frequency
U	Fluid Velocity
C_D	Drag Coefficient
C_L	Lift Coefficient
S	Blade Spacing
b	Blade Chord
α	Air Angle
$\frac{1}{2} U^2$, Q	Dynamic Head
$\mathcal{L}$	Lift
D	Drag
τ	Empirical Time Constant
S	Entropy
t	Time

Subscripts

Q. S.	Quasi-Steady
c	Compressor System
b	Blade
m	Mean
T	Stagnation Condition
1	Inlet
2	Exit

SUMMARY

Loss in compressor stall margin due to inlet flow distortion depends upon the amplitude, the radial and circumferential extent, and the duration of the distortion. Effects of amplitude and extent are adequately accounted for by distortion indices derived from correlations of steady, long duration distortions. This report addresses the problem of distortion duration. In particular, it is desirable to know the smallest duration time for which there will be a significant compressor response. This duration is defined as the critical response time.

Non-steady flow effects are dependent upon the travel time required for fluid movement through the compression system. For this reason, critical response time has been related to the time required for fluid to travel a distance which is significant for distortion sensitivity. This is conveniently expressed as reduced frequency: - the non-dimensional ratio of fluid travel time to the period of the distortion. Non-steady response was investigated in detail on two axial length scales, the blade length and the compressor length. Mathematical models were employed to ascertain which length scale controls the distortion sensitivity of the compressor. One of these models allows the investigation of unsteady response on the blade length scale. The other model is capable of including non-steady effects on the compressor length scale alone or on both scales simultaneously.

It was determined that, while non-steady effects on a blade length scale are important for long duration inlet distortion sensitivity, the compressor length scale sets the limiting duration time. Furthermore, the maximum reduced frequency at which a compressor is sensitive based upon compressor length was determined to be in the range of 1 to 5. Limited test data was used to further refine this estimate for critical reduced frequency to approximately 2.0.

INTRODUCTION

Engine inlet flow distortion is, in general, a complex combination of spatial and temporal variations in pressure, temperature and flow angle. Currently, the engine's response to a complex inlet distortion can be determined with confidence only by experiment. Some measure of success has been achieved by constructing distortion indices or factors, but these depend upon the assumption that the distortion (a combination of radial and circumferential variation) persists for a time period significant to the engine. That is to say, even though the spatial distortion is being altered as a function of time, it is assumed that the engine response is the same as if the distortion were time invariant. It is known, however, that as the duration time of a distortion diminishes, the engine's response necessarily also diminishes. This is because of the finite time required for the fluid as well as any flow disturbance to propagate through the engine's compression system.

The reliability of distortion indices can be improved if the required duration time is known for a particular compression system. This distortion duration can be defined as the "critical response time" for the compression system. Several investigators have successfully used this concept to improve the application of distortion indices, either through the use of a low pass analog filter(1) or, equivalently a digital running average for a specified averaging time(2) to evaluate inlet data. These two approaches can be related by the fact that the cut-off (-3dB point) frequency of the analog filter is equal to approximately one half of the inverse of the averaging time(3).

This artificial filtering of inlet pressure fluctuations is considered to be analogous to the natural falloff in the sensitivity of the compressor to these fluctuations at high frequency levels, see Figure 1. Better data filters could be constructed if the reduction in compressor sensitivity with frequency were known.

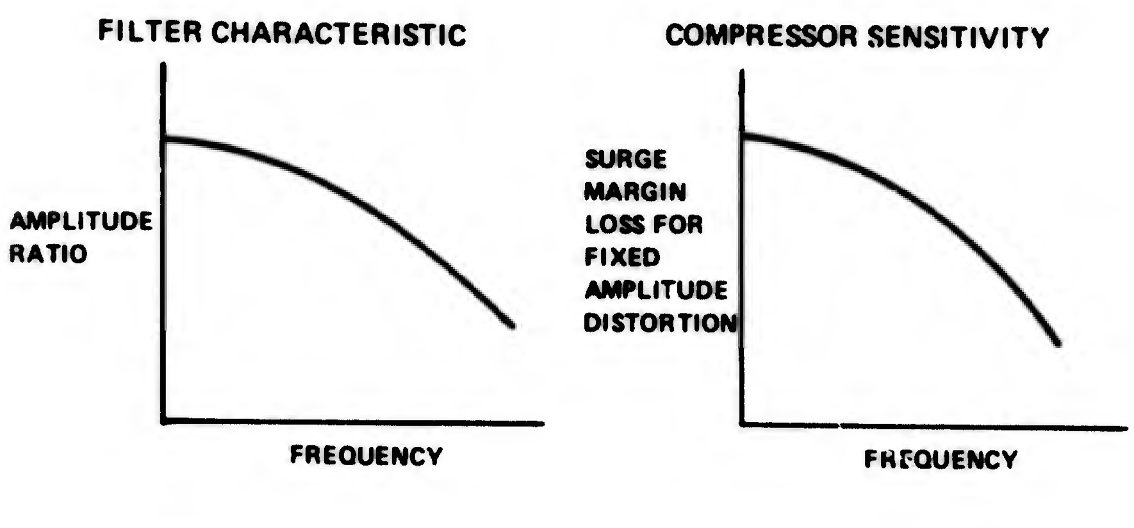

Figure 1 Similarity of Compressor Sensitivity to Analog Filtering

Preceding page blank

Consequently, a mathematical model capable of predicting the falloff in sensitivity of the compression system would be useful for determining the proper filter characteristic for the evaluation of inlet distortion data. Such a model is being developed at Pratt & Whitney Aircraft. This model is based upon the solution of the time dependent equations of motion using the Method of Characteristics (MOC). The MOC calculation is based upon the physical phenomenon of pressure wave and fluid particle propagation and, as such, does not suffer from phase problems normally associated with "lumped volume" models. A limitation of this model had been the use of quasi-steady compressor performance characteristics to represent the action of the compressor blades on the fluid. Under this contract, this limitation has been removed through the incorporation of non-steady blade loss effects. The non-steady blade loss calculation is based upon a rotor loss correlation derived from compressors operating with steady circumferential distortion. The use of this correlation is possible because the flow field is non-steady in the rotor reference frame even though the distortion is steady in the absolute sense.

This report details the work done under this contract to modify the P&WA MOC model to include non-steady blade losses. It includes a description of the basic technical approach and justification for the use of the rotor loss correlation. It details how the rotor loss correlation was obtained from the steady circumferential distortion data using a P&WA circumferential distortion model. The manner in which the loss correlation has been incorporated into the MOC model is described, and results of a three-stage compressor test case are presented.

Descriptions of the P&WA MOC model and the P&WA circumferential distortion model used in the non-steady loss correlation are included in separate appendices.

TECHNICAL APPROACH

Reduced Frequency

When a time unsteady phenomenon occurs, its significance depends upon the system under consideration. More specifically the frequency of the phenomenon (or inversely, its period) must be compared with the time required for fluid to traverse the system from its inlet to its exit. Reduced frequency has been defined in such a manner:

$$R.F. = k \frac{L \cdot F}{U}$$

where L = system length (ft)

F = disturbance frequency (Hz)

U = fluid velocity (ft/sec)

k = constant coefficient (normally equal to π)

It is appropriate to consider various magnitudes of reduced frequency. In order to do this, a typical compression system will be defined as follows:

Overall Length	$L = 2$ ft
Blade Length	$L_b = 0.2$ ft.
Fluid Velocity	$U = 600$ ft/sec

Depending upon whether we look at the entire compression system or an individual blade, the reduced frequency will differ by a factor of ten (one order of magnitude).

$$(R.F.)_c = \frac{\pi \cdot 2 \cdot F}{600} = .01 \cdot F$$

$$(R.F.)_b = \frac{\pi \cdot 0.2 \cdot F}{600} = .001 \cdot F$$

When a disturbance has a small reduced frequency (on the order of .01) the system can be expected to respond in a quasi-steady manner. That is, the response will be the same as if the disturbance took place at an infinitely slow rate. For the two systems under study, a reduced frequency of .01 corresponds approximately to:

$F = 1$ Hz (Compression System)

$F = 10$ Hz (Blade Row)

At the other extreme a large reduced frequency (on the order of 10) signifies a situation when the disturbance is varying so rapidly that the system has only a very limited response. This is understandable because the disturbance has fluctuated between its maximum and minimum values many times before the fluid can traverse the system. With a reduced frequency of 10, the two systems have approximately:

$F = 1000$ Hz (Compression System)

$F = 10000$ Hz (Blade Row)

Between these two extremes lies the area of interest when the system's time unsteady response is considered. The fact that the blade row system is actually part of the compression system further complicates the question concerning the relative significance of a time unsteady phenomenon. For example, at the upper frequency boundary of 1000 Hz (R.F. = 10) for the compression system, fluid flow velocity fluctuations at any point within the compression system will be of relatively low amplitude (attenuated). Thus, the response of the blade row system to these velocity fluctuations will necessarily also be of relatively low amplitude even though the reduced frequency for this system is approximately 1.0. Although compressor instability will be initiated by a breakdown of flow within the blade row system, it is probable that critical response time is set primarily by the compression system upper frequency, 1000 Hz or less in this example. In order to understand how the blade row system response modifies the critical response time, it is necessary to look at this system in detail.

Compressor In Steady Flow

Each rotor and stator in a compressor consists of a cascade of airfoils. Similar to an isolated airfoil, the performance of a cascade can be expressed in terms of lift and drag forces. The lift forces, being normal to the mean flow direction turn the fluid while the drag forces are in opposition to the mean flow direction and retard the fluid. These forces are normally expressed in terms of non-dimensional coefficients times mean flow dynamic head times area:

$$\mathcal{L} = C_L \cdot \rho \frac{Um^2}{2} \cdot A$$

$$D = C_D \cdot \rho \frac{Um^2}{2} \cdot A$$

The cascade parameters of importance are the blade-to-blade spacing(s), the chord length (b), and the mean flow angle (α_m) as well as the flow angles entering and leaving the cascade (α_1 and α_2). See Figure 2.

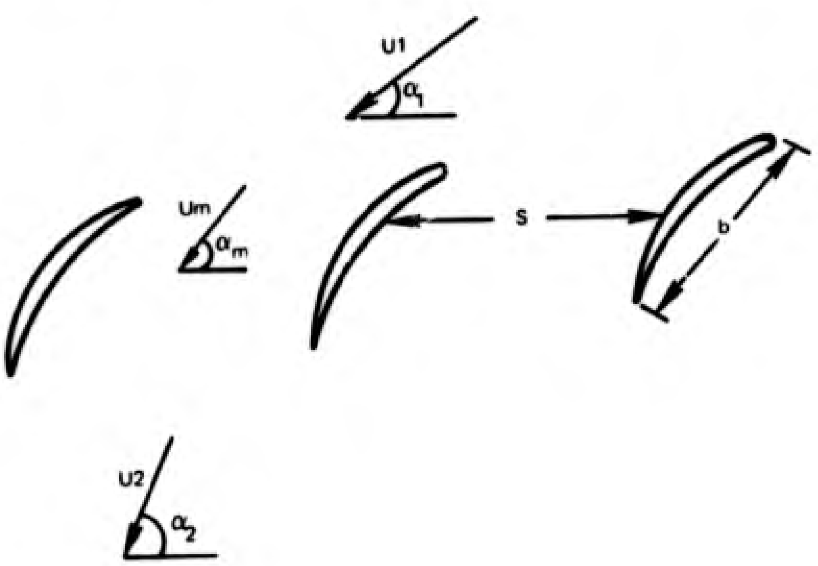

Figure 2 Cascade Parameter Identification

In reference 4 it has been shown that $C_L \simeq 2\frac{S}{b}(\cot\alpha_1 - \cot\alpha_2)\sin\alpha_m$

and $C_D \simeq \frac{S}{b} \cdot \frac{\Delta P_T}{\frac{1}{2}\rho U_1{}^2} \cdot \frac{\sin^3\alpha_m}{\sin^2\alpha_1}$

where ΔP_T is the measured loss in total pressure across the cascade. For a given geometry, the cascade solidity (s/b) and stagger angle (α_m) are fixed. It is therefore convenient to look at the cascade performance in terms of the change in air angle (turning) and total pressure loss . These parameters are related to the inlet air angle in the same manner that isolated airfoil lift and drag coefficients are related to incidence. The inlet air angle, as defined by P&WA nomenclature, is related to incidence angle according to Figure 3.

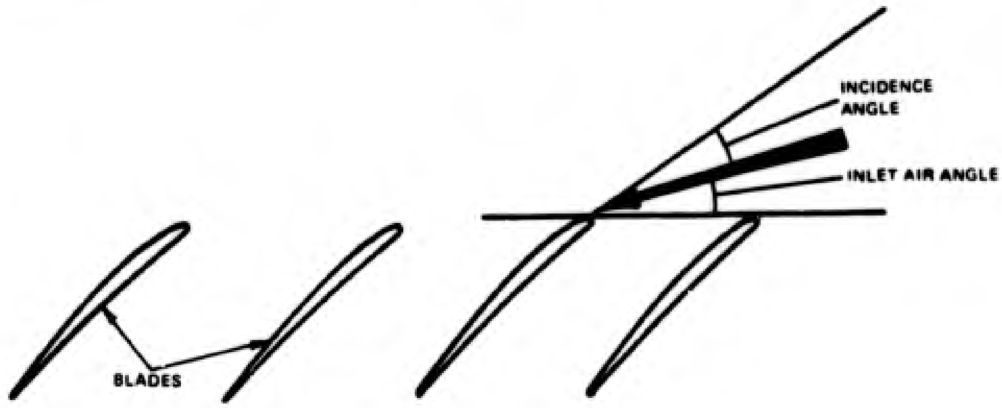

Figure 3 Inlet Air Angle Definition

The equivalent isolated airfoil and cascade performance parameters are shown in Figure 4.

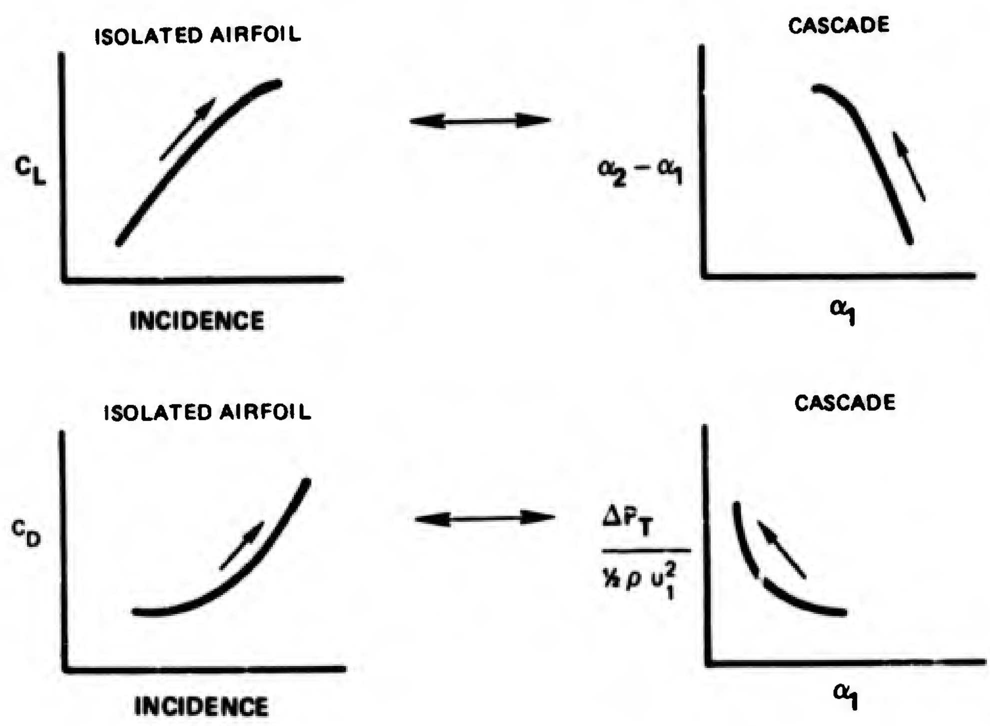

Figure 4 Isolated Airfoil and Cascade Performance Parameters

The reduction in lift and the increase in drag at high values of incidence occur because the fluid separates from the airfoil. The initial separation takes place near the airfoil trailing edge and moves towards the leading edge as incidence increases until the entire airfoil is separated or stalled. A similar sequence takes place in the cascade. Additionally, while a cascade is normally considered stationary, the same parameters apply to a rotor with the pertinent flow parameters evaluated in the rotating reference frame.

The P&WA models use measured static pressure rise and total temperature rise as a function of inlet corrected flow rate to represent blade row performance. Blade loss is represented by the entropy rise which can be calculated from the pressure and temperature rise. This representation is used because static pressures and total temperatures are directly measurable in a compressor test with fixed instrumentation while blade losses must be calculated from the results of detailed instrumentation traverses. The latter type of measurements are normally available from cascade testing but are not always obtained during a compressor experiment.

Compressor In Non-Steady Flow

If the incidence angle of an airfoil changes with time, the lift and drag coefficients will vary in some manner. When the rate of change of incidence is slow enough these coefficients assume the steady flow value. The term "quasi-steady" is an appropriate description of this response. This means that the lift and drag coefficients at any point in time are of essentially the same value they would have if incidence was not varying, but was fixed at the instantaneous value. If the incidence varies more rapidly, the lift and drag coefficients will deviate from the quasi-steady values as shown in Figure 5.

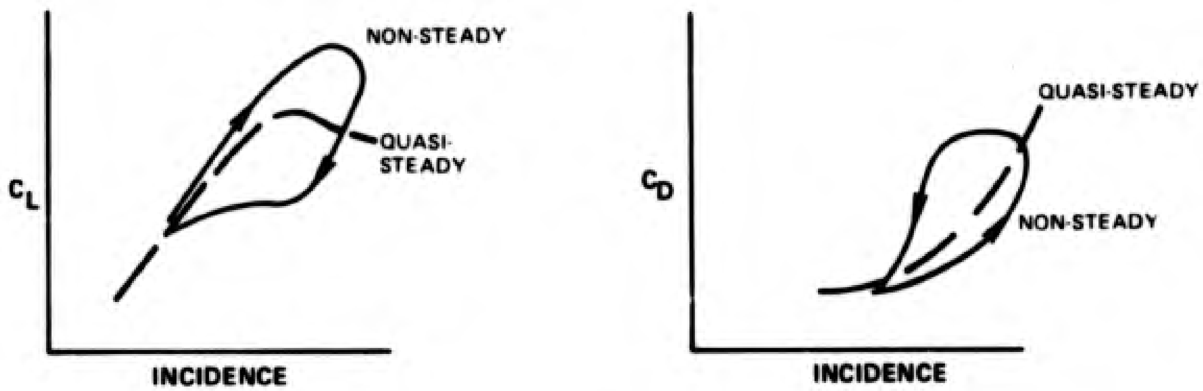

Figure 5 Unsteady Deviation of Lift and Drag Coefficients

The lift and drag coefficients for the non-steady case differ from the quasi-steady values at high incidence because of the finite time required for airfoil separation to develop. Whether the separation progresses from the trailing edge to the leading edge or occurs as an abrupt leading edge separation, it has been experimentally observed that a vortex-like disturbance is shed which passes over the airfoil at a convection velocity on the order of 1/3 to 1/2 of the free stream fluid velocity.(5) Similarly, experiments conducted with a cascade demonstrated that the separation point moves along the blade at a rate proportional to the time required for a fluid particle to move across the blade row.(6)

This experimental evidence makes it clear that a time unsteady flow analysis which relies on the quasi-steady blade row performance is necessarily limited in the accuracy of its results. The complexity of the non-steady separation process is not amenable to purely analytical treatment. Consequently it is necessary to correlate the non-steady loss and turning through a combined experimental/analytical procedure. In this way pertinent design parameters can be varied in a systematic way to ascertain their relative influence on the non-steady flow processes.

On the basis of the experimental observations of the boundary layer separation process, a simple model can be proposed which relates the non-steady performance to quasi-steady performance in the following manner:

$$\frac{d\,\text{Loss}}{dt} = \frac{1}{\tau}\left(\text{Loss}_{Q.S.} - \text{Loss}\right) \tag{1}$$

$$\frac{d\,\text{Turning}}{dt} = \frac{1}{\tau}\left(\text{Turning}_{Q.S.} - \text{Turning}\right) \tag{2}$$

These relations, stated simply, say that the rate at which loss and turning change with time is governed by how much they lag their quasi-steady counterparts (for the same value of inlet air angle). The term τ is an empiricaltime constant which is to be evaluated on the basis of blade row cascade geometry and pertinent flow variables. The experimental evidence suggests that

$$\tau = K\,(b/U) \tag{3}$$

where: K is proportionality constant to be determined

b is blade chord length
U is fluid velocity

The questions to be resolved are:

(1) Does this simple model approximate the non-steady flow?

(2) How do the pertinent cascade parameters such as solidity (ratio of blade chord to spacing), aspect ratio (ratio of blade span to chord) and loading level (level of static pressure rise across blade) influence the proportionality constant?

These questions must be resolved experimentally, but extensive testing of a compressor, or even a cascade, with time variant inlet conditions (eg. sinusoidally varying inlet total pressure) is a complex and expensive undertaking. It would be necessary to measure blade inlet and exit air angles and loss transiently with high response instrumentation, and then compare non-steady and quasi-steady values. For this reason, an alternate approach was taken which makes use of available test data.

These data are derived from compressor experiments with an imposed inlet total pressure circumferential distortion. One of these experiments was conducted with a single stage machine using high response instrumentation to measure rotor loss and turning. The remaining experiments were conducted with three stage compressors using only conventional instrumentation to measure overall compressor response. The overall response of these compressors to steady circumferential pressure distortion, of course, is different from the response to time variant inlet pressure fluctuations. The rotor blades, however, experience time variant changes in inlet air angle as they rotate around the circumference in the same manner that a stationary cascade would experience changes in a time variant flow field.

While the majority of the available circumferential distortion data is taken with conventional instrumentation, P&WA has an analytical model with the capability of calculating compressor response with either quasi-steady or non-steady blade response. This model is the multiple segment parallel compressor model, a detailed description of which appears in Appendix A. The model makes use of individual performance characteristics for each rotor and stator blade row. The performance of stators is quasi-steady since they experience a steady flow field. The rotors, however depend not only on local air angle but also on the way in which air angle changes with circumferential position (analogous to time in rotating reference frame). The model is capable of calculating the non-steady performance of rotors through the use of an appropriate time constant. This capability allows one to predict distorted compressor performance using a range of time constants, and thereby select the value which most closely approximates the data.

The demonstration of this capability has been accomplished using the single stage experimental results which include an indirect measurement of the time constant. These experimental results are depicted graphically in Figures 6 and 7. These figures show the measurements of rotor loss and exit air angle, respectively, in quasi-steady and non-steady flow. We will now consider Figure 6 in more detail. This figure shows rotor blade losses measured on a compressor rig using high response instrumentation. The measurements were made both with a steady uniform inlet and a 180° circumferential distortion screen. The uniform inlet data was obtained by measuring the rotor blade wakes at different values of rotor inlet angle. The air angle was reduced (incidence angle increased) by throttling the compressor discharge until the compressor stalled. The circumferential distortion data was obtained at one throttle position by measuring the inlet air angles and rotor blade wakes at different positions around the circumference.

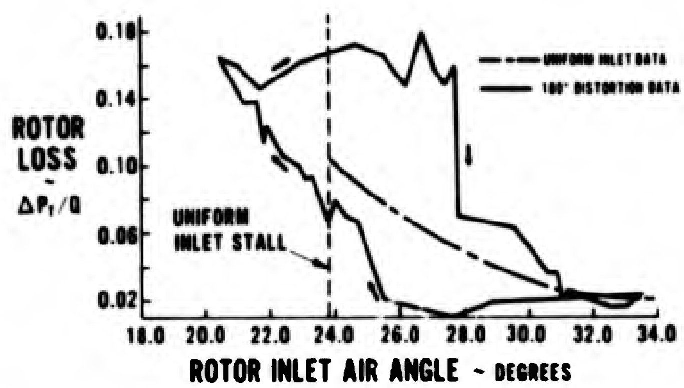

Figure 6 Rotor Response to Inlet Air Angle – Experimental Data

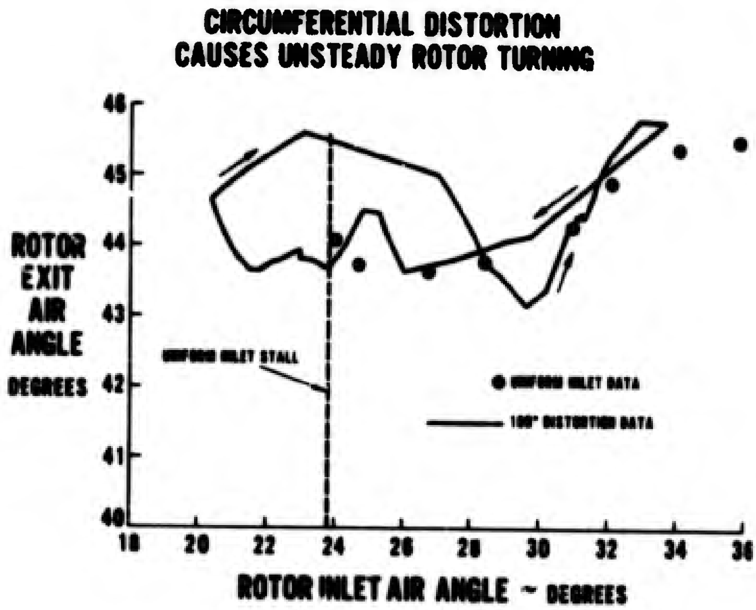

Figure 7 Unsteady Exit Air Angle Measurement – Experimental Data

In this way, one full cycle of rotor blade loss for a single revolution was obtained. Starting at a high inlet air angle (away from the distortion screen) the rotor moves behind the screen (in direction of arrows) and inlet air angle is reduced. The measured blade loss, however, lags behind the uniform inlet data. Before emerging from behind the screen, the rotor blade experiences air angles lower than the values at the uniform inlet stall point, but does not stall. This is similar to lift and drag coefficient data for a typical airfoil as shown in Figure 5. The rotor finally emerges from behind the screen, again lagging behind the uniform inlet loss until the cycle has been completed. If the first order loss model described by equation (a) is correct, it should be possible to calculate the circumferential distortion loss data with an appropriate time constant. This has been done for the data of Figure 6 and reasonably good agreement was obtained for a value of time constant, $\tau = 1.0$ b/u, as shown in Figure 8.

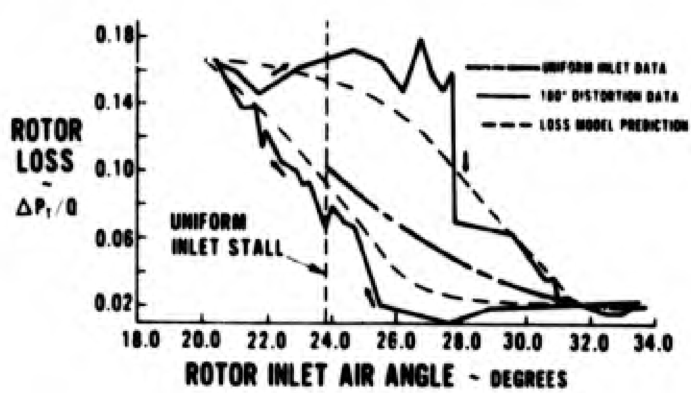

Figure 8 Rotor Response to Inlet Air Angle – Experimental Data and Prediction

A similar evaluation was attempted using the measured exit air angle data. It was found, however, that it was not possible to define a single value for the time constant which could approximate the data. In order to avoid additional complexity and on the basis of the observed small variation in exit air angle (approximately 1.5 degrees), the decision was made to use quasi-steady turning and non-steady losses in the multiple segment model to predict distorted performance. The good prediction of the distorted compressor stall point shown in Figure 9 justifies the decision for this compressor. Furthermore, in a high solidity cascade, the variations in exit air angle with inlet air angle are relatively small. The general application of the quasi-steady turning is therefore not considered to be a serious limitation to the non-steady calculations.

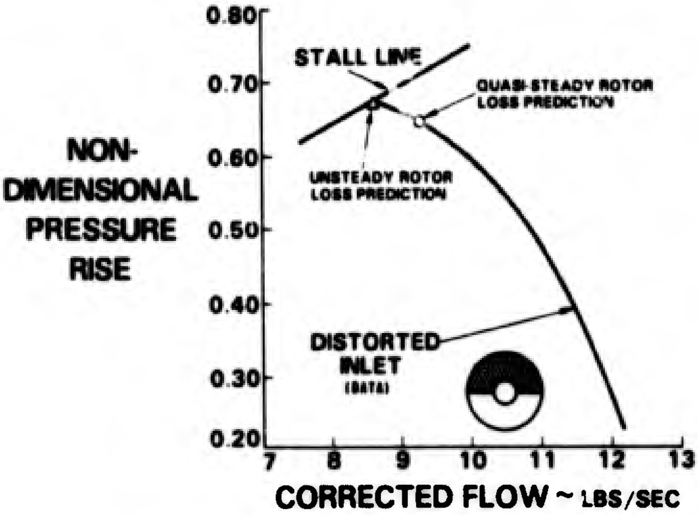

Figure 9 Multi-Segment Model Compressor Stall Predictions

The approach selected is therefore one which uses available test data and analytical techniques to define a general procedure for the evaluation of non-steady blade loss. This procedure may then be applied to the method of characteristics model to evaluate its impact on the response of a compressor to a time variant distortion.

TIME CONSTANT DETERMINATION

The basis for the general determination of the non-steady loss proportionality constant is P&WA's multiple segment parallel compressor model. As explained in Appendix A, it is possible to differentiate various distorted flow phenomena using this model. This capability makes it possible to predict a compressor's response to circumferential distortion with various rotor blade loss assumptions. The quasi-steady loss may be directly applied as derived from local flow conditions and blade row performance curves. Additionally, a form of equation 1 may be used to calculate losses in the non-steady rotating frame of reference.

The time constant in equation 1 may be systematically varied to ascertain its effect on the model predictions. The results of model calculations can be evaluated in two ways. First of all a prediction of the mass flow rate at the distorted stall point can be compared with experimental measurements. Secondly the circumferential distribution of airflow at the stall point can provide an appraisal of the loss calculation. The relative agreement between model predictions and experimental data is the basis for selecting the proper value of the time constant. Using the model in this manner, the time constant can be determined for a representative number of compressor configurations.

Selection of Circumferential Distortion Data

A large data bank of circumferential distortion data was available. In order for this circumferential distortion data to be useful for defining the influence of cascade parameters on non-steady blade losses, it had to:

1) Cover a wide range of pertinent cascade parameters (aspect ratio, solidity and loading level)

2) Include a systematic change in the cascade parameters so that the effect of each one could be evaluated individually.

3) Consider a range of circumferential extents of the distorted region to verify general applicability of the unsteady loss model.

4) Have sufficient instrumentation to provide an accurate evaluation of the distorted flow parameters around the circumference.

Data which satisfy these requirements were available from a series of three stage compressor rig experiments. Distortions of various extents were generated for these tests using a perforated steel plate located ahead of the compressor. Measurements of flow rate, static pressure, total pressure, total temperature and flow angle were made at a number of axial and circumferential locations. In addition, the distortion plate was continuously rotatable so that data measurements could be made at different circumferential locations relative to the distortion. A cross section of the test rig showing typical instrumentation is provided in Figure 10. A summary of the three stage compressors is shown in comparison with the base single stage compressor in Table 1.

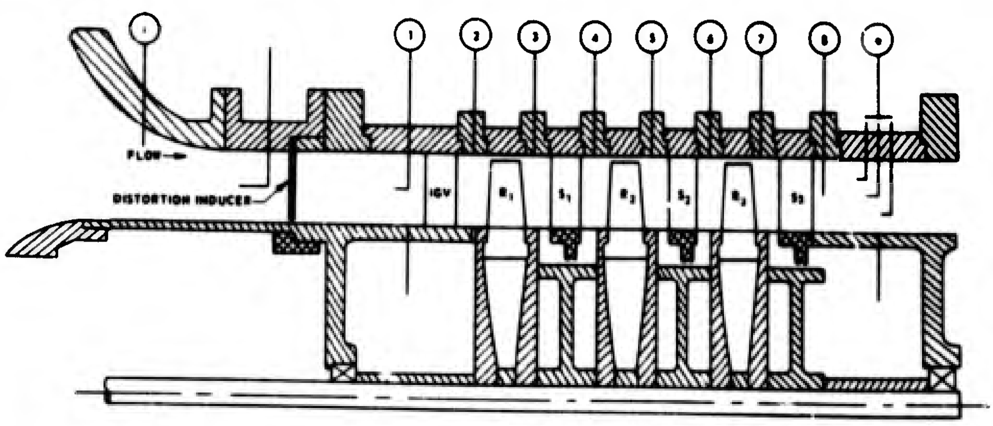

Figure 10 Three-Stage Compressor Test Rig Showing Instrumentation Stations

TABLE 1 COMPRESSOR DISTORTION COMPARISON

Configuration	# Stages	Average Rotor Aspect Ratio	Average Rotor Solidity	Average Radial Loading ($\Delta P/q$)	Distortion Extents
1	1	2.0	1.2	.3	180
2	3	1.2	1.36	.4	60,90,180
3	3	.8	1.36	.4	60,90,180
4	3	1.0	1.36	.5	60,90,180

Calculation Procedure

Having defined the compressor configurations to be used in determining the unsteady loss time constant, it was first necessary to establish an adequate representation of quasi-steady blade performance for each compressor. This was done primarily on the basis of undistorted, uniform inlet test data covering a range of airflow rates from maximum to stall. However, the multi-segment model requires the quasi-steady row performance characteristics of the compressor for the range of flows passed through the various circumferential segments. Unsteady flow effects associated with circumferential distortion allow some segments to operate at flow levels below the undistorted stall point. Blade row performance at these low flow rates cannot be obtained from the undistorted compressor data. An alternate procedure must be used for defining blade row performance in this flow regime. Consequently, performance curve extrapolations were predicted using a cascade correlation based upon mean-line blade geometries. Together with the steady-state unstalled data, the extrapolations were used to create a continuous row performance curve (Figure 11) by extending the curve through the data roughly parallel to the cascade prediction. (In general, cascade predictions do not match steady-state data exactly because of span-wise geometry and flow variations.)

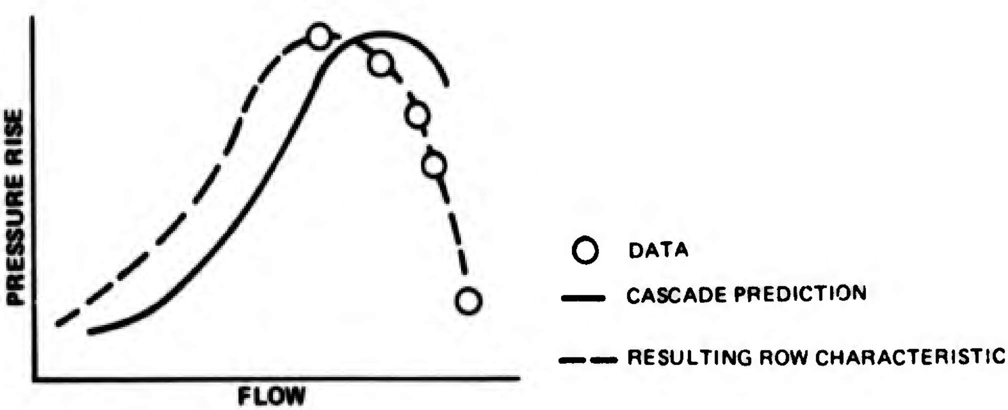

Figure 11 Extrapolation of Steady State Row Performance Data

To improve the level of the extrapolated curves, data from the region of low flow from a near-stall distorted inlet case were examined. Data from a small circumferential section behind the screen (approaching the screen trailing edge in the rotational direction) show flow rates below the undistorted stall flow. These data also exhibit minimal unsteady effects in the rotors as noted by a relatively flat inlet flow velocity curve, Figure 12. Utilizing the initial extrapolations, the distortion model was used to predict the circumferential position of low flow segments representing this region (those with small values of pressure rise attributable to unsteady effects) at the leading edge and trailing edge stations of each blade row. The particular low-flow segments were then traced back through the compressor, and the data measured at these circumferential positions were used to generate equivalent steady-state points on the row performance curves. The model was also used to estimate any residual unsteadiness, which was subtracted from these points for the rotor blades. These data points, always of a limited flow range, were used to extend the range of the performance curves into the stalled region as shown in Figure 13. In determining the final curve, these low flow points were weighted more heavily than the cascade prediction.

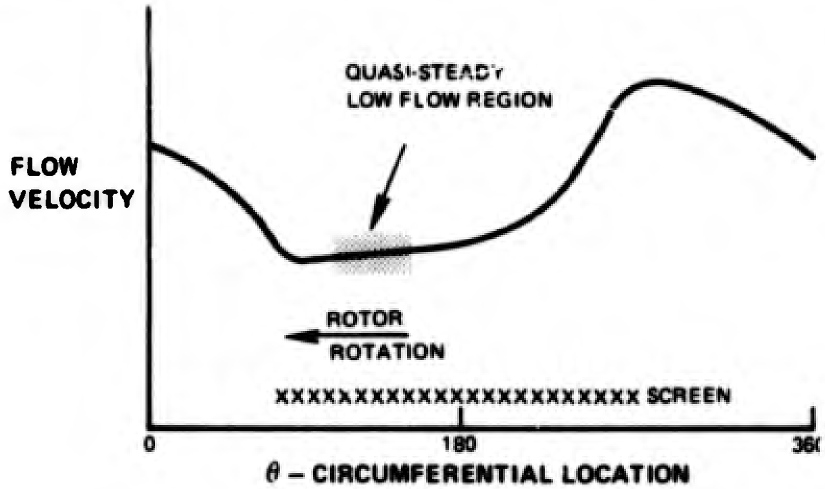

Figure 12 Circumferential Region of Low Unsteady Effects

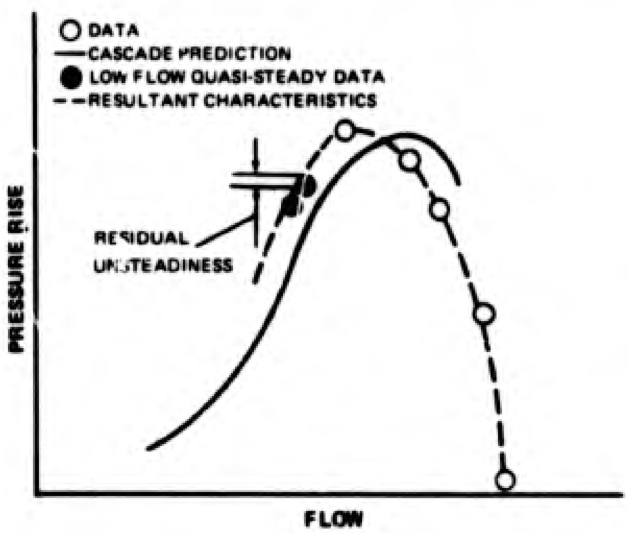

Figure 13 Adjustment of Extrapolated Region

The distortion data analysis was begun by using the results of the single stage compressor described earlier which indicated that the time constant was approximately equal to the time required for the fluid to move from the rotor leading edge to the rotor trailing edge, i.e. the loss lag proportionality constant was 1.0. The requirement was to determine whether the proportionality constant was always approximately 1.0 or whether it changed from one compressor configuration to another. The procedure which was followed for each of the three stage configurations consisted of the following steps:

1. The data from 180° distortion extent testing was predicted for each compressor with a proportionality constant equal to 1.0.

2. If the results when a value of 1.0 was used did not agree with the data, the proportionality constant was varied in an attempt to improve this agreement.

3. The same procedure was then repeated using the 60° and 90° extent distortion data.

The model was run using 36 individual segments, each representing a circumferential region 10° in width. The large number of segments provides an accurate description of the non-uniform inlet total pressure profile.

A typical inlet total pressure profile is shown in Figure 14. The non-square shape of the distortion occurs because the distortion screen is located close to the compressor inlet plane. The inlet flow which does not pass through the screen has a uniform total pressure level, but the total pressure of the fluid passing through the screen varies with the velocity at which it passes through the screen. The airflow velocity at the leading edge of the distorted region remains higher than the average flow in this region because of unsteady effects, and consequently the loss through the screen in this region is greater.

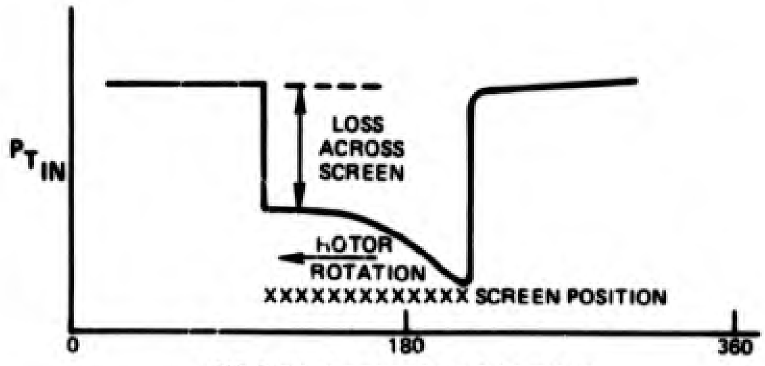

Figure 14 Typical Inlet Pressure Profile

The measured inlet total pressure profiles were input to the multiple segment model program, together with the other measured boundary conditions: exit static pressure profile and uniform inlet temperature. The model then predicted the mass flow rate at stall and the airflow distribution which satisfied these boundary conditions. The resulting inlet static pressure profile was then compared with the data at the measured stall airflow. In general, the predictions for the mass flow rate at stall did not match the data (see Table 2) exactly. Since this was observed, the measured stall flow rate was specified, and the model's prediction of airflow distribution at this flow rate was compared with the data. In the instances where the model predicted a stall airflow higher than that indicated by the data, it was not possible to run the model at the measured stall airflow. In these cases the airflow distribution from the predicted stall point was compared with the data.

TABLE 2

Comparison of Measured Stall Performance with P&WA Model Predicted Performance Using Rotor Loss Lag Proportionality Constant K = 1.0

Configuration	Distortion Extent	Measured Flow at Stall	Predicted Flow at Stall	Measured Pressure Ratio at Stall	Predicted Pressure Ratio at Stall
2	60	14.88	14.61	1.32	1.316
	90	14.56	14.80	1.32	1.318
	180	14.47	14.65	1.32	1.327
3	60	14.50	14.81	1.329	1.348
	90	14.07	14.44	1.314	1.339
	180	13.60	14.35	1.311	1.342
4	60	14.55	13.66	1.377	1.396
	90	14.17	13.60	1.365	1.388
	180	13.72	13.76	1.370	1.385

Results

Measured compressor performance parameters are compared in Table 2 to P&WA circumferential distortion model predictions which were made using a rotor loss lag proportionality constant of 1.0. Stall point flow rates were predicted with greater accuracy with the rotor loss lag proportionality constant K=1.0 than with K=0. However, the lack of consistency in the results indicate that stall point prediction alone was not adequate for defining the rotor loss lag proportionality constant. Variation of the proportionality constant to improve the prediction for a given configuration and distortion extent resulted in a random distribution of values which did not correlate with changes in geometry. This problem can be understood by considering the basis for the prediction of stalling airflow. The stall criterion is based upon the solution at which some segment has reached its peak pressure rise as determined from the blade row performance curves and calculated unsteady pressure rise across rotors. In the region near stall the slope of the exit static pressure vs airflow is very shallow, making a small error in pressure rise result in a significant airflow variation. Because the major component of the pressure rise is achieved from extrapolated blade row performance curves, the predicted stall point is very sensitive to the extrapolations. Even though great care was taken using cascade correlations and distortion data at low flow rates to calculate the extrapolations, they were not satisfactory for predicting the exact stall point.

The primary method for evaluating the proportionality constant was therefore based on the comparison of the circumferential flow distribution predictions with the test date. The flow distribution produced by the compressor operating with total pressure distortion can be inferred from measured inlet static pressure distributions. The predicted inlet circumferential static pressure profiles based on input measured total pressure profiles are compared to the measured static pressure profiles in Figures 15 through 23. Unless specifically noted otherwise, a rotor loss lag proportionality constant of 1.0 was used for the predictions.

Two measured pressure profiles appear in Figures 18 thru 23. The square symbols represent data taken at the near stall condition. The circles represent more extensive data resulting from rotation of the distortion screen. These data were taken at flow conditions further removed from the stall point to preclude inadvertent stall before screen rotation was completed. Rotation provides better resolution of the pressure profiles which can then be used to aid in the interpolation of the shape of the profile between the squares.

Ideally, the loss lag proportionality constant would be that value which resulted in perfect agreement between model prediction and measured data. Perfect agreement is unlikely, due to flow redistribution within the compressor and other effects which may not be completely accounted for in the model. Referring back to Figure 6, the greatest deviation between quasi-steady and non-steady rotor loss occurs where, having reached a minimum value, the air angle increases. Since the air angle is at a minimum value, this is the most likely location for unsteady loss to influence the compressor stability. This location corresponds to the region where the rotor has just entered the undistorted sector of inlet flow. Agreement between the predicted value of inlet stall pressure gradient when compared with the measured value in this region was the basis of selection of the rotor loss proportionality constant because this gradient was fairly sensitive to the value of this constant.

Figures 15, 16, and 17 show very good agreement of inlet static pressure profile for configuration 2 at 60, 90, and 180 degree extents of distortion, respectively. A loss lag proportionality constant of 1.0 was therefore considered applicable to configuration 2. This good agreement indicates that the proportionality constant is not significantly influenced by cascade parameters since aspect ratio, solidity and loading level for this configuration are all different than the base single stage configuration.

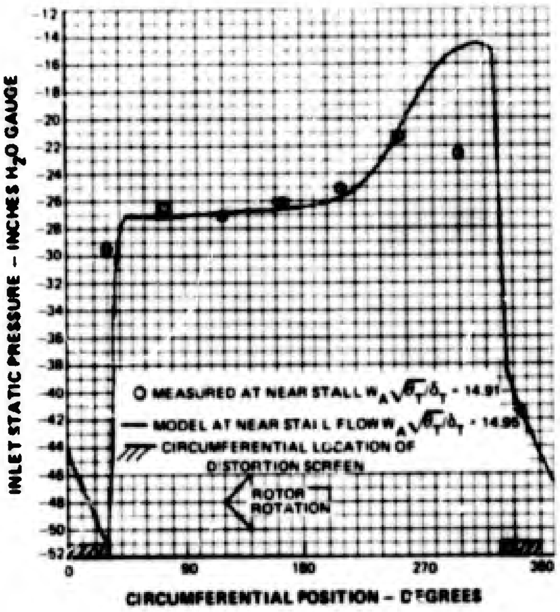

Figure 15 Circumferential Variation of Inlet Static Pressure Configuration 2-60° Screen

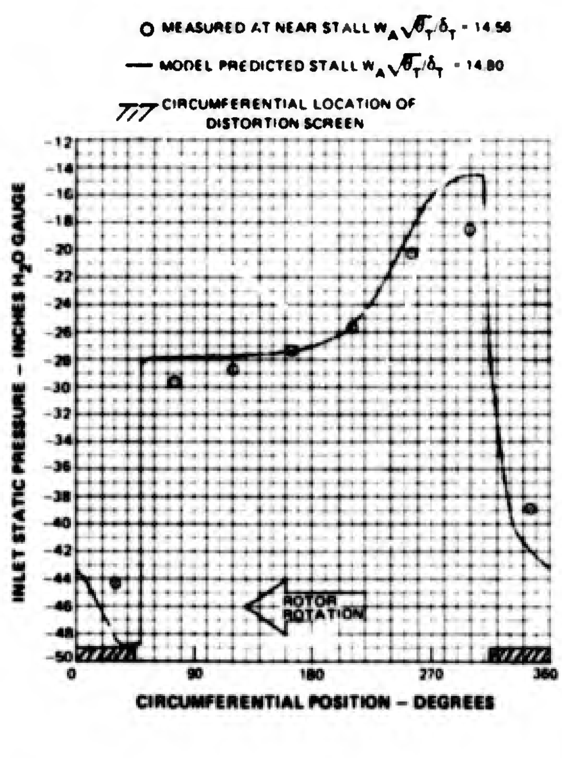

Figure 16 Circumferential Variation of Inlet Static Pressure Configuration 2-90° Screen

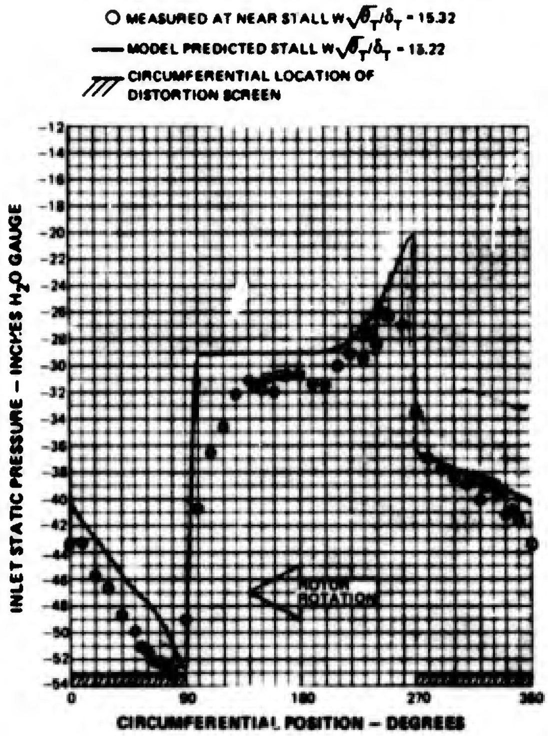

Figure 17 Circumferential Variation of Inlet Static Pressure Configuration 2-180° Screen

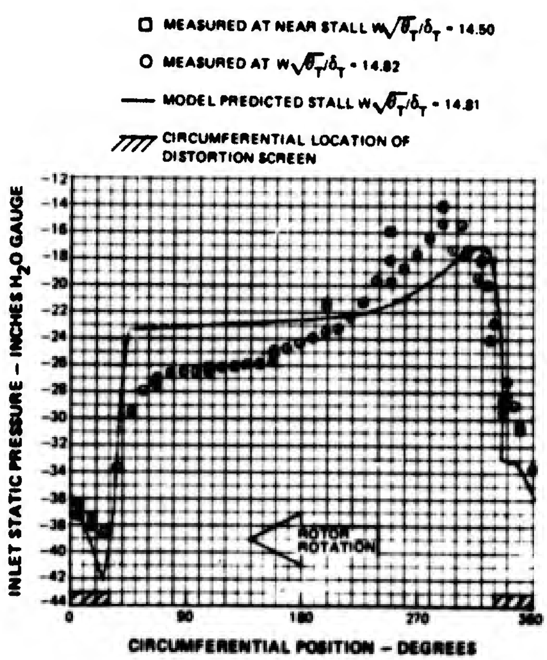

Figure 18 Circumferential Variation of Inlet Static Pressure Configuration 3-60° Screen

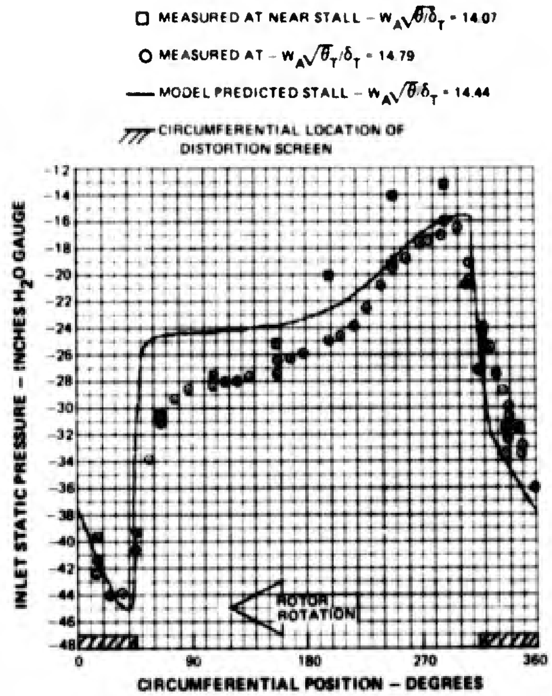

Figure 19 Circumferential Variation of Inlet Static Pressure Configuration 3-90° Screen

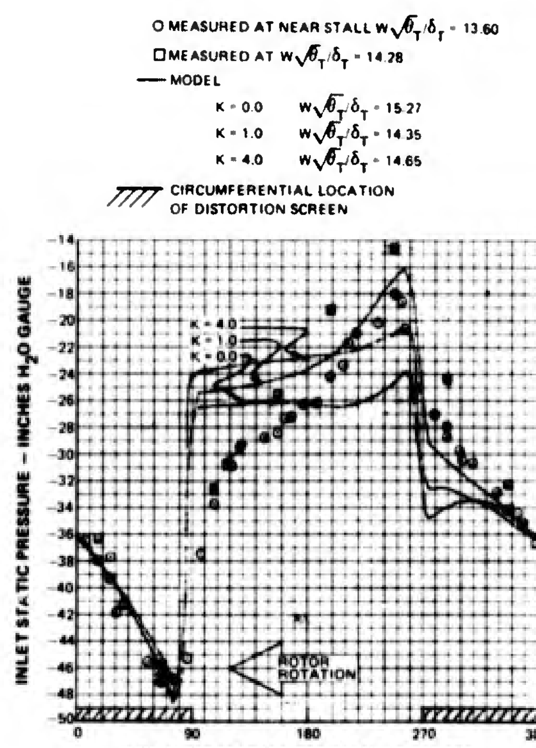

Figure 20 Circumferential Variation of Inlet Static Pressure Configuration 3-180° Screen

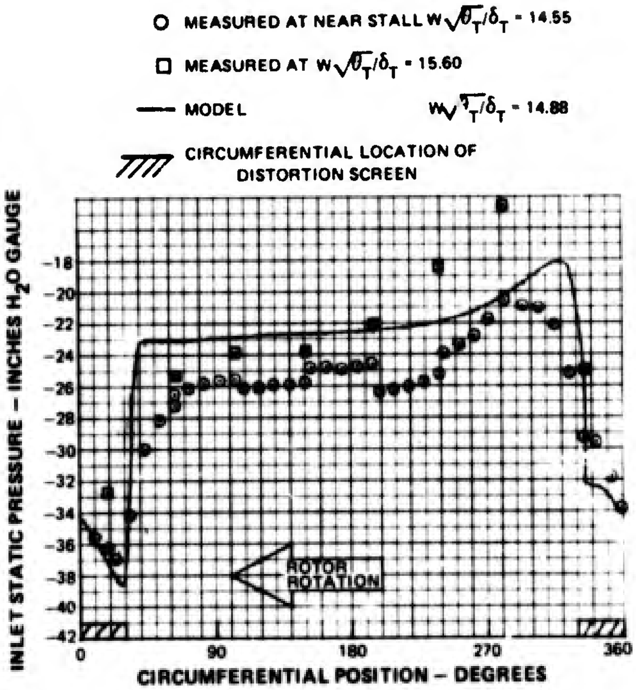

Figure 21 Circumferential Variation of Inlet Static Pressure Configuration 4-60° Screen

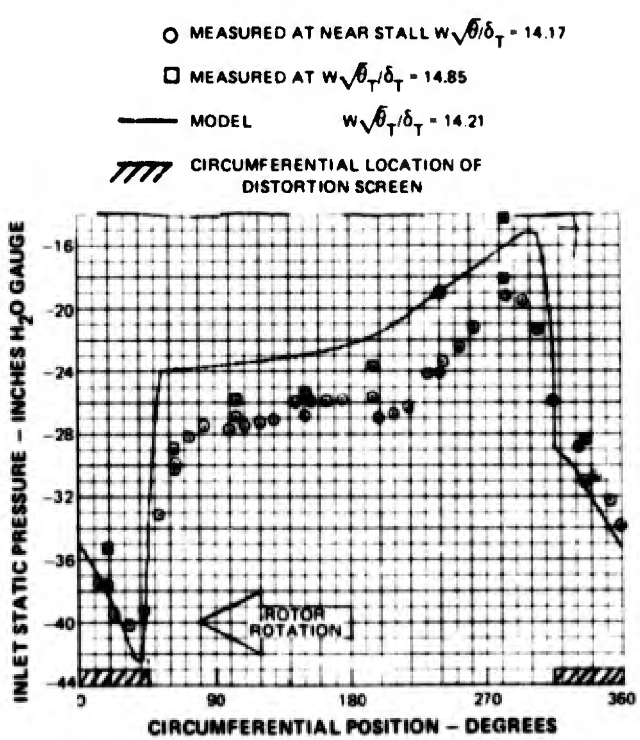

Figure 22 Circumferential Variation of Inlet Static Pressure Configuration 4-90° Screen

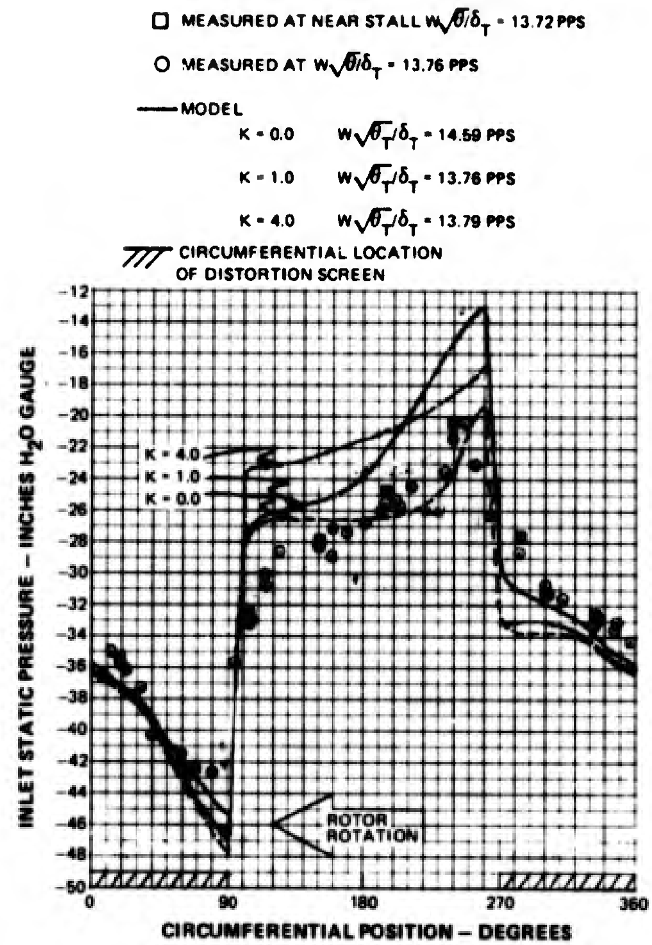

Figure 23 Circumferential Variation of Inlet Static Pressure Configuration 4-180° Screen

Agreement between the P&WA model and data is not quite as good for configuration 3 as shown in Figures 18, 19 and 20. Where there is a pressure plateau predicted by the model there remains a decreasing pressure gradient in the data as the rotor approaches the distorted region. The comparison on Figure 20 includes additional loss lag proportionality constants of 0.0 and 4.0. The plateau also persists with these values which means some factor other than unsteady loss response is responsible for the disagreement. As previously mentioned, the most likely place for unsteady loss to influence the compressor is in the region where the rotor is entering the undistorted region. The proportionality constant of 1.0 is clearly superior to 0 and 4.0 in this region in Figure 20. Again a loss lag proportionality constant of 1.0 or possibly a little less, was concluded to represent configuration 3. Rotor aspect ratio is the only difference between configurations 2 and 3 and, again, does not have a strong influence.

Configuration 4 has a higher loading level than the other configurations and is presented in Figures 21, 22 and 23. In this configuration the plateau noted as a difference between P&WA model predictions and data is present in both the data and in the model prediction. However, the steeper gradient of the static pressure data in the region where the rotor is entering the undistorted region indicates that the loss lag proportionality constant is near but less than 1.0. In Figure 23 the inlet static pressure profiles for loss lag proportionality factors of 0.0 and 4.0 have also been included. Inspection of Figure 23 indicates that a proportionality constant near 1.0 is correct, but the scatter of the data in the region entering the undistorted region precludes defining a more precise number. There was also some uncertainty in the measured airflow rate at stall for this point which is demonstrated by the level difference between the prediction and the data.

Although the model results have provided only an approximation of the proportionality factor, there is obviously no large influence of the cascade design parameters. For this reason, a single value of rotor loss lag proportionality factor of 1.0 was selected for use in the time unsteady method of characteristics model. This value, within the ability to differentiate, is the consensus of the effort under this contract, earlier P&WA high response measurements, and the results of other investigators[6][7].

MODIFICATION OF METHOD OF CHARACTERISTICS MODEL

The basic P&WA method of characteristics model assumes that the action of the compressor blades on the fluid may be represented by the quasi-steady compressor performance maps. This model is described in more detail in Appendix A. Under this contract the MOC model has been modified to account for non-steady blade losses in evaluating compressor performance. This means that the blade loss or entropy rise across a blade row is not just dependent upon the local instantaneous flow conditions. It is additionally influenced by the time history of entropy rise across the blade row.

$$\frac{\partial \Delta Sc}{\partial t} = \frac{1}{\tau}\left(\Delta Sc_{Q.S.} - \Delta Sc\right) \tag{1}$$

In order to illustrate how this effect is implemented, let us consider an instant of time t at which the contribution of the compressor blades to the flow field is to be evaluated. Flow conditions at the inlet to the blade row are used to evaluate the pressure and temperature rise in the normal manner. From these flow properties, the quasi-steady entropy rise is calculated $\Delta Sc_{Q.S.}$. The non-steady entropy rise is then determined:

$$\frac{\partial \Delta Sc}{\partial t} = \frac{\Delta Sc(t) - \Delta Sc(t-\Delta t)}{\Delta t} = \frac{1}{\tau}\left(\Delta Sc_{Q.S.}(t) - \Delta Sc(t)\right)$$

$$\Delta Sc(t)\left(\frac{1}{\tau} + \frac{1}{\Delta t}\right) = \frac{\Delta Sc_{Q.S.}(t)}{\tau} + \frac{\Delta Sc(t-\Delta t)}{\Delta t}$$

$$\Delta Sc(t) = \left(\frac{\tau \Delta t}{\tau + \Delta t}\right)\left(\frac{\Delta Sc_{Q.S.}(t)}{\tau} + \frac{\Delta Sc(t-\Delta t)}{\Delta t}\right) \tag{2}$$

The non-steady loss only alters the pressure rise since the total temperature rise is determined solely from the work input of rotor blades, which is assumed to be equal to the quasi-steady value, or is zero across stator blades. The pressure rise must be recalculated from the non-steady entropy rise and the temperature change. This provides the necessary information to evaluate the blade force and blade loss functions in the time unsteady solution of the equation of motion.

Compressor Test Case Calculation

The three stage 2.0 aspect ratio compressor was chosen for the test case evaluation of the non-steady blade loss. An average flow condition was chosen approximately 10% above the quasi-steady stall airflow. This point was chosen so that a significant inlet total pressure oscillation could be imposed without causing an instability indicative of compressor stall. In order to check the significance of the non-steady loss calculation it is also necessary to be operating over a flow range with a significant range of quasi-steady blade loss. With an inlet total pressure variation of ±0.5 times inlet dynamic head ($1/2\ \rho U^2$), the test case satisfies both of these requirements, except at the lower frequencies (< 20 Hz) where it was necessary to reduce the inlet total pressure variation to ±.1 times inlet dynamic head to avoid an instability. The response of the test compressor was evaluated with the MOC model over a frequency range from 10 Hz to 200 Hz, which covers a reduced frequency range based upon compressor length of .5 to 10. The limiting case of a quasi-steady disturbance was also evaluated manually to provide a range for the compressor from a quasi-steady response through solutions where the compressor response is quite small.

The questions of interest are:

1) What is the limiting frequency above which the compressor response is insignificant?

2) Does the non-steady blade response significantly alter the limiting frequency or is it governed primarily by non-steady flow effects on the compressor scale?

In order to evaluate the relative response of the compressor at different frequencies the attenuation of the flow disturbance was investigated. This was done in terms of the amplitude of the compressor mass flow variation and the attenuation of the inlet disturbance through the compressor. The mass flow variation has been normalized by the amplitude of the inlet total pressure variation. The attenuation is determined from a ratio of total pressure variation at the exit to that at the inlet. Results of the MOC model are presented using both a quasi-steady and a non-steady loss calculation in Figures 24 and 25. From these figures, it is apparent that, while the blade loss assumption does alter the solution in the frequency range of interest, the dominant effect is the reduction of the mass flow variation at high frequency.

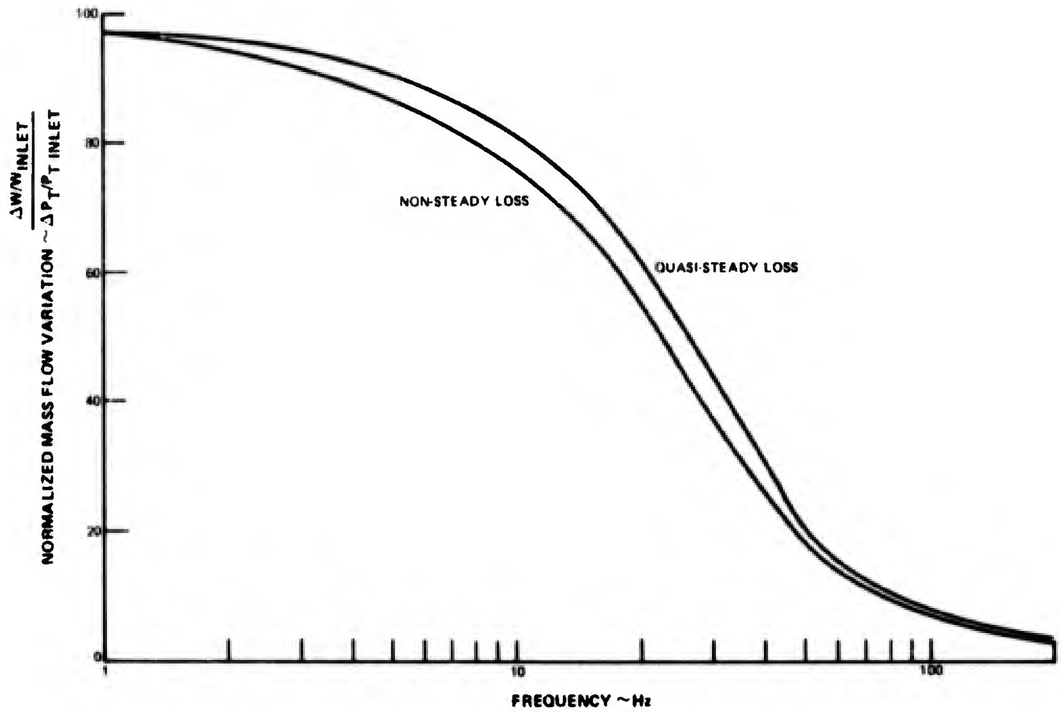

Figure 24 Variation of Mass Flow with Disturbance Frequency

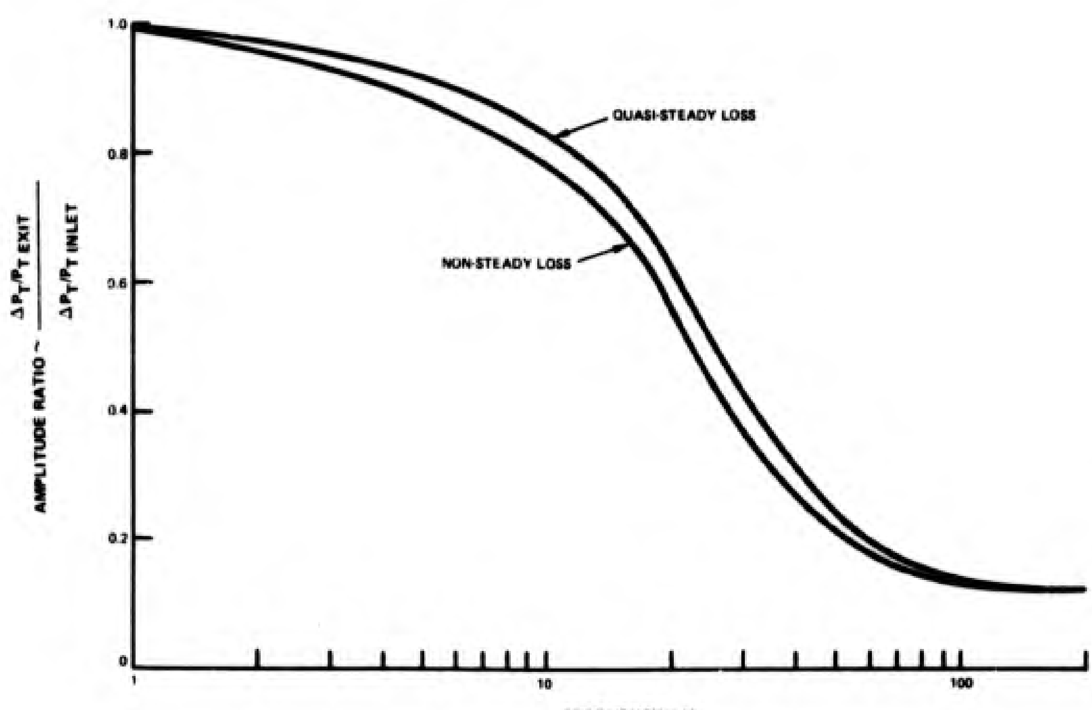

Figure 25 Effect of Disturbance Frequency on Attenuation

The limiting frequency for a significant compressor response cannot be determined precisely from these results, but it is possible to specify a probable range. Clearly, the response above 100 Hz (compressor reduced frequency = 5.) is not significant and sets the upper limit to this range. The lower limit must be set somewhat arbitrarily. It is most likely in excess of 10 Hz because the mass flow variation has only diminished by approximately 20% from the low frequency value. The compressor response at 20 Hz is still greater than half the quasi-steady level so it is probable that the critical frequency lies in the range of 20 Hz to 100 Hz. This corresponds to a reduced frequency range of 1 to 5.

A survey of published data can be used to gain some additional insight into the critical level of reduced frequency. Time variant inlet distortion testing was reported in reference 1 and relates the sensitivity of a fan plus low pressure compressor. It was determined that the sensitivity to time variant distortion of this machine at design speed was well correlated if the inlet data were filtered using a 160 Hz. low pass analog filter. The reduced frequency for this machine at 160 Hz. and be calculated:

$$\text{R.F.} = \frac{\pi \cdot 2.9\ \text{ft} \cdot 160\ \text{Hz}}{700\ \text{ft/sec}}$$

$$\text{R.F.} = 2.08$$

In order to make the significance of this number understood, the amplitude ratio characteristic of a 160Hz (3 pole) filter is shown in Figure 26. At high frequencies the filter reduces the amplitude of inlet pressure fluctuations which are used to calculate a distortion index. This reduced amplitude distortion index is then used to estimate the resultant loss in stall margin based upon a correlation of steady, time invariant distortion data. The successful use of this technique implies that the natural reduction in compressor distortion sensitivity is similar to the filter's artificial reduction in distortion amplitude. Whether or not this is a valid conclusion was investigated to some extent in Reference 8. In this report, similar results for filter cut-off frequency were obtained by other investigators using independently generated time variant distortion data for the same compression system. It was also determined in this work, however, that the "rolloff" rate in amplitude ratio above the cutoff frequency was only of secondary importance. One therefore concludes that the falloff in compressor sensitivity is quite rapid above this cutoff-frequency. It should be noted, however, that the critical value of cutoff frequency was defined using a rather coarse mesh (50 Hz) of filter frequencies to reduce the distortion data. On a reduced frequency basis, this corresponds to an uncertainty of ±1.0 in the investigated flow range. Hence, a lower filter cutoff frequency might have yielded equally satisfactory results, but may have been more sensitive to rolloff rate above the cutoff frequency. The major point to be concluded, however, is that this compression system is insensitive to complex, time variant inlet distortions above a reduced frequency of 2.0. This is consistent with the MOC model results which suggest that critical reduced frequency is between 1.0 and 5.0.

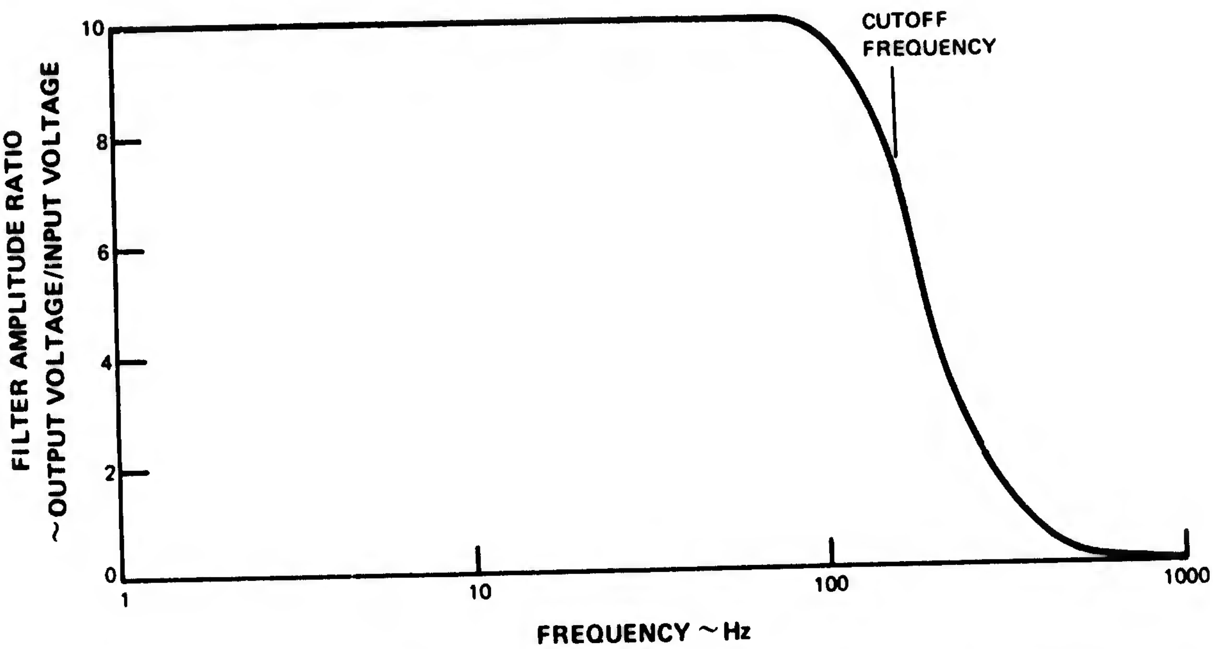

Figure 26   Attenuation Characteristics of a 160° Hz (3-pole) Filter

The practical application of the critical reduced frequency concept is the establishment of analog filter cutoff frequency or digital averaging time for the analysis of time dependent distortion data. While it is not likely that the very sharp rolloff in typical filter characteristics matches the actual falloff in compressor sensitivity, it is apparently adequate if the cutoff frequency is approximately equal to the frequency at which compressor response is a minimum. On the basis of these limited results it appears that filter cutoff frequency can be limited to a reduced frequency range of 2.0 with a good probability that compressor sensitivity will be satisfactorily correlated. Similarly an averaging time should be used which corresponds to one half of the period at the reduced frequencies in this range. These guidelines are summarized below:

Analog Filter

$$\text{Cutoff Frequency (Hz)} = \frac{2.0 \cdot \text{Fluid Velocity (Ft/Sec)}}{\pi \ . \ \text{Compressor length (ft)}}$$

Digital Averaging

$$\text{Averaging Time (Sec)} = \tfrac{1}{2} \ . \ \frac{\pi \ . \ \text{Compressor Length (Ft)}}{2.0 \cdot \text{Fluid Velocity (Ft/Sec)}}$$

CONCLUSIONS AND RECOMMENDATIONS

The following conclusions can be drawn from the results of work under this contract:

1) Reduced frequency is the controlling parameter for non-steady compressor response to inlet flow distortion.

2) Reduced frequency on the blade length scale is most significant for compressor response to circumferential inlet distortion which does not vary with time. Other blade cascade parameters examined (blade aspect ratio, solidity and blade loading) do not influence the non-steady blade response.

3) Reduced frequency on the compressor length scale is the significant parameter for determining critical response time for time variant inlet distortion.

4) Results of a mathematical model of a compressor's transient response indicate that the critical reduced frequency based on compressor length is between 1.0 and 5.0.

5) Limited test data demonstrates that the critical reduced frequency is approximately 2.0.

As a continuation of this effort the following is recommended:

1) The general applicability of the limiting value of reduced frequency (2.0) should be tested against available distortion sensitivity data. It should be compared with filter cutoff frequency levels or averaging time values which have successfully correlated such data.

2) Alternatively, the P&WA mathematical model based on the method of characteristics could be used to predict compressor sensitivity to time variant inlet conditions. This would require verification of the model using data from an experiment with discrete frequency pulsation of inlet pressure. Once verified the model predictions could be used to evaluate the limiting reduced frequency for a range of compressors for comparison with the value of 2.0. Model results could also be used to improve filter characteristics at high frequency.

3) Until such verification is completed, it is recommended that the reduced frequency of 2.0 be used in establishing preliminary values for filtering inlet distortion data.

4) Further analysis relating distortion sensitivity to reduced frequency should be made as suitable compressor data becomes available.

REFERENCES

1. Plourde, G. A. and Brimelow, B., "Pressure Fluctuations Cause Compressor Instability", Proceedings of the Air Force Airframe Propulsion Compatibility Symposium, June, 1969.

2. Brimelow, B., Collins, T.P., and Pfefferkorn, G.A., "Engine Testing in a Dynamic Environment", AIAA Paper No. 74-1198, AIAA/SAE 10th Propulsion Conference, October, 1974.

3. Moore, M.T. and Lueke, J.E., "A Similarity Parameter for Scaling Dynamic Inlet Distortion", Transactions of the ASME, Journal of Engineering for Industry, August, 1974.

4. Shepherd, D.G., Principles of Turbomachinery, MacMillan Company, New York, 1956.

5. McCroskey, W. J., Carr, L.W., and McAlister, K.W., "Dynamic Stall Experiments on Oscillating Airfoils", AIAA Paper 75-125, AIAA 13th Aerospace Sciences Meeting, 1975.

6. Weinberg, S.L. and Heiser, W.H., "Use of Hydrogen Bubble Technique in Observing Unsteady Boundary Layers, ASME Paper 68-FE-33, 1968.

7. Nagano, S., Machida, Y., and Takata, H., "Dynamic Performance of Stalled Blade Rows", Japan Society of Mechanical Engineers, Paper June 11, 1971.

8. King, R. W., Schuerman, J.A. and Muller, R.G., "Analysis of Distortion Data from TF30 P-3 Mixed Compression Inlet Test", NASA CR-2686, 1976.

APPENDIX A – CIRCUMFERENTIAL DISTORTION MODEL

Parallel Compressor Theory

Parallel compressor theory considers the circumference of the compressor to be divided into two flow regions: one of relatively low velocity such as would exist behind a distortion inducing screen and one of relatively high velocity. The essential points of parallel compressor theory are illustrated in Figure A-1. The compressor performance in each region is assumed to be that obtained from uniform flow operation at the local value of inlet velocity. It is further assumed that circumferential crossflow within the compressor is negligible and that the exit static pressure is uniform. The total pressure distortion is attenuated by the compressor because of the difference in pressure ratio between the high and low velocity regions. In addition, a temperature distortion is created out of phase (high temperature-low pressure) with the pressure distortion due to this attenuation. The limit of stability (stall point) of the distorted compressor is predicted to occur when the low velocity region reaches the uniform flow (undistorted) compressor stall point. The resultant performance at stall is calculated as the area average of the two regions.

Multiple Segment Parallel Compressor Model

The current model expands the basic parallel compressor theory by using multiple parallel segments to provide a detailed definition of the circumferential flow field. These segments pass through the compressor from inlet to exit. They do not, in general, enter and exit the compressor at the same relative circumferential location, but swirl to some degree commensurate with blade stagger angles, rotor rotation, and propagation characteristics of the flow properties assumed for the model and discussed in the following section. The flow rate in each segment is determined from its boundary conditions (inlet total pressure & total temperature and exit static pressure) and the compressor's performance within that segment in a manner quite similar to classic parallel compressor. The concept of using multiple parallel segments, however, is much more complex than the multiplication of the classic calculation. The complexity arises from two dimensional flow effects and from unsteady flow effects caused by the relative motion of rotor blades through the distorted flow region.

Consider a circumferential segment as it approaches the compressor. In the presence of a non-uniform inlet total pressure, circumferential static pressure gradients exist at the compressor inlet which redistribute the flow and can alter the flow velocity and direction of that segment. The performance of the first blade row will depend on the local flow angle as well as the local inlet flow rate within the segment. Proceeding through the compressor, the circumferentially non-uniform static pressure can cause further flow redistribution, particularly when "stagnant" air cavities exist external to the compressor flow path. This redistribution will result in a different amount of airflow in the segment at different axial locations within the compressor. When the segment encounters a rotor blade row, unsteady flow effects must be accounted for due to the circumferential nonuniformity of the flow field. The rotor performance depends not only on the local flow velocity and incidence but the time dependent (in the rotating reference) velocity and incidence gradients it experiences as it rotates past the segment.

Finally, the exit static pressure may not be uniform so it is necessary to know the angular displacement of the segment as it traverses the compressor in order to apply the proper downstream boundary condition. None of these effects are considered by basic parallel compressor theory but are all accounted for in the multiple segment model. The only restriction to the multiple segment approach is that the circumferential extent of the segment should span several blade passages. The flow properties in each segment are then representative of local average conditions. This restriction poses no problem as long as the distortion is large relative to the blade pitch or spacing, which, as previously stated, covers most cases of practical interest.

A further departure from parallel compressor theory is the use of individual blade row performance on the premise that deviations from uniform inlet performance will result in changes to the front-to-rear matching of the compressor blade rows. Such changes cannot be easily assessed on the basis of an overall performance representation. However, regardless of the way in which the uniform inlet performance is presented, the important point is to recognize the deviations from this performance that can occur under distorted flow conditions.

Procedurally, the multiple segment model calculation is similar to a classic two-segment parallel compressor solution. Each segment has known inlet and exit boundary conditions, and the mass flow rate consistent with these boundary conditions is to be determined. The major distinction is that the compressor segment performance is influenced by the distorted flow and is not identical to uniform flow performance as assumed by classic parallel compressor. In order to evaluate unsteady flow effects, the flow rates of adjacent segments are required in determining a given segment's performance. It is necessary, therefore, to establish a periodic solution around the circumference of the compressor. It is only after periodicity of mass flow rate is established that a calculation is considered complete. This is in contrast to the discontinuities in mass flow rate allowed by classic parallel compressor at the boundaries of the distorted region.

Calculation Procedure

Each segment has a constant circumferential extent with a fraction of the total mass flow entering the compressor. The fraction of the total mass flow in a given segment is dependent upon that particular segment's boundary conditions and the overall performance characteristic of the compressor for that segment. The performance characteristic effectively changes from segment to segment because of the various phenomena outlined in the previous section.

The inlet boundary condition for a segment is easily defined from the prescribed inlet total pressure and total temperature. The other boundary condition required is the static pressure at the exit of each segment. The average level of exit static pressure required to satisfy the specified total mass flow must be determined iteratively. Furthermore, the possibility of having non-uniform exit static pressure (Reference 1, for example) makes it necessary to know the proper circumferential location of each segment at the exit of the compressor.

Each segment moves circumferentially as it passes through the compressor since mean flow angles within the rotors, stators and gaps are seldom axial. In addition, the rotation of the rotor provides additional angular displacement. This is illustrated schematically in Figure A-2. Note that the segment displacement due to the rotor ($\Delta\theta$ segment) is less than that for a fluid particle ($\Delta\theta$ particle). This is because the acoustic path is important in establishing the non-steady flow in the rotating reference frame. Since an acoustical signal exceeds local fluid velocity in the forward direction, the "residence time" in the rotor is less than that for a fluid particle.

Angular Displacement = Residence Time x Angular Velocity

$$\Delta\theta_{\text{Segment}} = \left(\frac{b}{u+a}\right) \omega$$

or

$$\Delta\theta_{\text{Particle}} = \left(\frac{b}{u}\right) \omega$$

The angular displacement of each segment is calculated from local conditions and an average for all the segments is used to match proper inlet and exit boundary conditions. The average angular displacement of the segments is denoted as "flow swirl".

The compressor performance as well as the exit boundary conditions is therefore partially dependent upon the mass flow distribution. Consequently, an iteration scheme is utilized which necessarily assumes a mass flow distribution and solves for the mass flow in each segment on the basis of this assumption. The calculated mass flow distribution then replaces the original assumption and the procedure is repeated until the calculated mass flow distribution agrees with the assumed mass flow distribution. The necessity of knowing the mass flow distribution in order to calculate compressor performance will now be illustrated by a discussion of the various distorted flow phenomena incorporated in the multiple segment model.

Distortion Induced Inlet Flow Redistribution

Flow redistribution takes place upstream of a compressor operating with non-uniform flow as the compressor acts to create an upstream attenuation of the inlet flow distortion. A further description of this phenomenon may be found in Reference 2. The resultant inlet static pressure imbalance and a streamline curvature, Figure A-3, causes a variation in inlet air angle. With no inlet guide vane the incidence on the first rotor blade varies as in Figure A-4. The multiple segment model calculates this inlet angle variation in order to properly determine the first blade row performance.

The procedure for calculating the upstream flow redistribution is based on the use of a distribution of sources and sinks at the compressor inlet plane to represent the effect of the compressor on the upstream flow. As the fluid approaches the compressor, the axial velocity distribution is altered from the values far upstream of the compressor. In some regions around the circumference the fluid velocity is decreased as it gets closer to the compressor so that a flow source opposing this fluid may be thought to exist. Similarly, a flow sink would account for an increase in the velocity of the fluid as it approaches the compressor. The strengths of these sources and sinks are calculated in the following manner.

The upstream velocity distortion is separated into its rotational and irrotational components, both of which are considered to have amplitudes such that a linearized description can be adapted. The rotational component is associated with the inlet total pressure distortion. Since the total pressure is convected by the flow from far upstream to the compressor, the rotational velocity distortion can be evaluated far upstream ($-\infty$) where the irrotational component is zero.

$$\delta C_{X_{ROT}} = \delta C_{X_{-\infty}} = \frac{1}{\rho \bar{C}_X} \frac{\delta P_{O_{-\infty}}}{\left(1+\frac{\gamma-1}{2}\bar{M}^2\right)^{\frac{\gamma}{\gamma-1}}} \qquad (\delta P_{S_{-\infty}} = 0)$$

The irrotational part of the velocity distortion is due to the upstream flow redistribution induced by the compressor. Since there are multiple segments, the compressor can be represented by an array of sources and sinks located at the compressor inlet plane with the effect of compressibility accounted for by using a Prandtl-Glauert transformation. The local strength of the source (sink) is calculated from the irrotational component of axial velocity at the inlet.

$$\delta C_{X_{IRROT}} = \delta C_{X_{INLET}} - \delta C_{X_{ROT}}$$

The inlet velocity distortion, $\delta C_{X_{inlet}}$, is a function of the compressor performance and local boundary conditions for each segment and is determined iteratively. The source (sink) strengths determined from $\delta C_{X_{irrot}}$ can be used in a formulation from Reference 3 to determine the velocity potential function for such an array. The tangential velocity perturbation component can then be determined from this potential function. It should be noted that although the analysis has been derived on the basis of small perturbations, comparison with measured data shows that the calculation has provided an accurate solution for the inlet air angle distribution even when the imposed inlet total pressure distortion was quite large (see Figure 14).

Circumferential Crossflow

Circumferential flow redistribution can also occur within the compressor as well as upstream of it. Within the compressor, this flow redistribution can take two different forms as illustrated by Figure A-5. First of all, the compressor flowpath has axial gaps between blade rows which provide a means for redistributing the flow. This occurs primarily near the edges of the distorted region where static pressure gradients are largest. Since it is localized to the edges and since normal axial spacing in a modern engine is small, this form of cross-flow can normally be considered negligible, and is not included in this analysis.

The second form of cross flow can take place within cavities (roots of shrouded stators and bleed plenums) which are exposed to the circumferential pressure gradient. Since the static pressure differences can be large and the fluid within a cavity has negligible axial momentum, the crossflow can be significant. This was demonstrated qualitatively by a flow visualization experiment on a 3 stage compressor with inlet distortion, the results of which are shown in Figure A-6. In this experiment, felt tufts were mounted in an annular plenum external to the compressor flowpath. The tufts were viewed through a plexiglass cover and indicated substantial circumferential flow velocities consistent with the imposed pressure distortion.

The calculation procedure in the current model consists of an evaluation of mass flow transfer between each segment and the external flow cavity. The flowpath circumferential static pressure distribution is assumed to be known but the cavity pressure distribution must be determined iteratively. Since the crossflow occurs as a steady flow process there can be no mass accumulation within the cavity. Therefore, the solution for the static pressure distribution within the cavity must satisfy a continuity balance. The calculation depends upon the flow characteristics of the cavities as well as those of the passages connecting the cavities with the flowpath. Large cavities induce the most crossflow and for these the flow characteristics of the connecting passages are more significant than the cavity flow characteristics for determining crossflow rate.

In general, exact flow characteristics for these connecting passages are not available. The model makes use of a general correlation of flow coefficients for air being bled off perpendicular to the flow direction. This correlation was empirically derived in Reference 4 and is reproduced on Figure A-7. Because of the general nature of this correlation, the results of the current model are only approximate. However, the usual amplitude of crossflow within any single cavity is only a small percentage of the total airflow. The use of generalized flow coefficients is normally adequate.

The sequence of the iteration starts with a single segment (one having a relatively high flowpath static pressure is selected) by assuming the local static pressure within the cavity. Flow characteristics for the passage connecting the flowpath with the cavity are used to determine the mass transfer into the cavity. These characteristics depend upon the static pressure difference across the connecting passage, the cross-sectional area of the passage, and flow conditions (static pressure, total temperature, Mach number) on the high pressure end of the passage. The mass flow which enters from the first segment into the cavity is used to calculate the Mach number in the cavity, based upon the cavity geometry. Proceeding in the direction of rotor rotation to the next segment, a change in total pressure occurs due to the friction or drag of the cavity walls. These walls may be either stationary or rotating and the frictional losses depend on the relative flow velocities. The mass transfer calculation is repeated at the next segment based upon the local flow parameters. The mass flow rate within the cavity and the flowpath are appropriately adjusted and the calculation is continued until a full circuit around the circumference is completed. A check is then made for continuity of mass flow into and out of the cavity. If continuity of mass is satisfied within a preset tolerance the solution is accepted. If not, the calculation is repeated using a higher or lower guess for cavity pressure depending upon whether the net cumulative mass flow into the cavity is positive or negative. The iteration is continued until a solution (zero net mass flow into the cavity) is obtained.

Unsteady Flow Effects

Another reason why distorted performance differs from uniform inlet values is because the rotor experiences time variant changes in velocity and incidence as it moves through the distorted flow field. First of all, the acceleration of fluid through the rotor implies a local static pressure difference between the leading and trailing edges over and above that indicated by the quasi-steady pressure rise characterstic. This additional pressure rise must be accounted for in determining the distorted compressor performance.

In order to simply illustrate the basic fluid mechanics of this unsteady static pressure change across the blade row, the blade passage can be modeled in the rotating reference frame as a one-dimensional, inviscid, linear diffuser with unsteady flow.

For this one-dimensional inviscid diffuser, it will be assumed that area varies linearly from inlet to exit as illustrated in the figure below. The unsteady pressure change can be determined from application of the Momentum Equation.

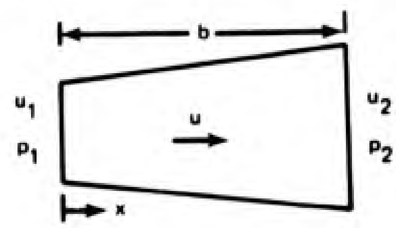

$$-\frac{1}{\rho}\frac{\partial p}{\partial x} = u\frac{\partial u}{\partial x} + \frac{\partial u}{\partial t}$$

$$-\int_0^b \frac{\partial p}{\partial x}\, dx = \int_0^b \rho u \frac{\partial u}{\partial x}\, dx + \int_0^b \rho \frac{\partial u}{\partial t}\, dx \qquad (1)$$

The first term on the right is the quasi-steady state pressure rise due to diffusion and is considered to be the static pressure rise across the blade row with uniform, time invariant inlet conditions. This term is evaluated like an actuator disk for the circumferentially local mass flow rate and combined with the second term which represents the effect of local acceleration of the fluid within the blade passage. For simplicity, this term will now be evaluated for the case of an incompressible fluid in order to indicate the controlling parameters. The effects of compressibility have been determined separately and are included in the computer model in an approximate manner. The circumferential displacement of the segment by the rotor provides for the proper acoustic delay of the static pressure rise.

Assumptions:

$$u_1 = \bar{u}_1 + u_1'$$

$$\frac{\partial u_1}{\partial t} = \frac{\partial u_1'}{\partial t}$$

$$u(x) = u_1 \frac{A_1}{A(x)}$$

$$A(x) = A_1 + \frac{A_2 - A_1}{b} x$$

Substituting into Equation 1

$$\int_0^b \rho \frac{\partial u}{\partial t} dx = \rho \int_0^b \frac{\partial u_1'}{\partial t} \frac{1}{1 + \frac{A_2 - A_1}{A_1 b} x} dx \qquad (2)$$

$$\int_0^b \rho \frac{\partial u}{\partial t} dx = \rho \frac{\partial u_1'}{\partial t} \underbrace{\frac{A_1 b}{A_2 - A_1} \ln \frac{A_2}{A_1}}_{\mathcal{L}}$$

$$p_2 - p_1 = \int_0^b \rho u \frac{\partial u}{\partial x} dx - \rho \mathcal{L} \frac{\partial u_1'}{\partial t} \qquad (3)$$

The unsteady part of the pressure rise is thus proportional to the rotor chord length and the change of relative inlet velocity. This acceleration rate can be determined from the fixed coordinate system velocity distortion and the rotational speed of the rotor.

In order to calculate the change in stagnation temperature due to this unsteadiness, the following relation between fluid properties, which may be derived from the First Law of Thermodynamics, is applicable:

$$T\,ds = dh - \frac{1}{\rho}\,dp \tag{4}$$

$$h_o = h + \frac{u^2}{2}$$

$$\therefore dh_o = dh + u\,du$$

$$T\,ds = dh_o - u\,du - \frac{1}{\rho}\,dp$$

Integrating across the diffuser:

$$\int_0^b T\frac{\partial s}{\partial x}\,dx = \int_0^b \left(\frac{\partial h_o}{\partial x} - u\frac{\partial u}{\partial x} - \frac{1}{\rho}\frac{\partial p}{\partial x}\right)dx \tag{5}$$

From Momentum Equation:

$$-\frac{1}{\rho}\frac{\partial p}{\partial x} = \frac{\partial u}{\partial t} + u\frac{\partial u}{\partial x}$$

$$\int_0^b \frac{\partial h_o}{\partial x}\,dx = -\int_0^b \frac{\partial u}{\partial t}\,dx + \int_0^b T\frac{\partial s}{\partial x}\,dx \tag{6}$$

Thus, the change in stagnation enthalpy relative to the rotor is composed of two terms. The first term corresponds to the unsteady pressure rise and will be treated by making the same assumptions concerning compressibility.

$$\int_0^b \frac{\partial u}{\partial t}\,dx = \mathcal{L}\,\frac{\partial u_1'}{\partial t}$$

$$T_{o2} - T_{o1} = -\frac{1}{C_p}\,\mathcal{L}\,\frac{\partial u_1'}{\partial t} + \frac{1}{C_p}\int_0^b T\frac{\partial s}{\partial x}\,dx \tag{7}$$

This unsteady total temperature rise is added to the steady rotor temperature rise as determined from uniform inlet flow conditions. The steady and unsteady total temperature rises are combined in a manner similar to the static pressure rise. Like the unsteady pressure rise, the unsteady temperature rise is proportional to the rotor chord length and the time rate of change of velocity relative to the rotor. Even though the analysis is an inviscid one, the second term is generally non-zero because of the entropy gradients associated with the upstream total pressure (or temperature) distortion. In order to properly account for the entropy gradients, it is necessary to know the path line followed by fluid particles through the compressor. The second term is evaluated for each segment using the difference between the circumferential displacement of a fluid particle and the circumferential displacement of the segment to define the amplitude of the entropy gradient. The temperature change so determined is then added to the steady and unsteady temperature change for each segment.

Fluid Particle Displacement Effects

It is necessary to calculate the fluid particle displacement because the particles within a rotor blade passage can swirl into and out of the distorted flow region. When viewed from a fixed reference frame, the entropy of the fluid entering a rotor passage may be different from that of the fluid leaving that same passage at that instant in time as shown in Figure A-8. This difference in entropy must be accounted for in calculating the changes in the temperature across the blade passage, as can be seen from Equation 7.

Since the flow process across the blade row was considered inviscid in this analysis, any entropy change across the blade row must be due to a difference in instantaneous inlet and exit fluid properties. This difference becomes evident when it is realized that fluid particles are displaced circumferentially by the rotor and that the fluid within the blade passage at any time originated from a circumferential sector of finite extent. The extent of this sector is a function of the rotational speed, the rotor chord length and the relative fluid velocity. The properties of the fluid leaving the rotor passage originated at the beginning of this sector while the entering fluid comes from the end of the sector. Thus, the entropy change across the rotor is equal to the circumferential entropy difference across the sector, which is easily defined from the imposed rotor inlet total pressure and total temperature distortion and the sector extent. The displacement of the fluid by each rotor blade row is calculated and accumulated in the multiple segment parallel compressor model in order to provide an accurate exit total temperature distortion profile.

This effect on total temperature due to particle displacement accounts for the observation often made with multistage compressors that the exit total temperature distortion is not aligned with the attenuated total pressure distortion as predicted by parallel compressor theory. This is illustrated in Figure A-9 where the exit total temperature distortion has been calculated from measured attenuation of an imposed inlet total pressure distortion. The agreement with data is greatly improved by accounting for particle displacement when calculating the temperature distortion.

The impact of particle swirl on distorted compressor stage matching is illustrated in Figure A-10. As shown in the figure for parallel compressor, the low total pressure region and high total temperature region are aligned throughout the compressor. Note that in this particular example no circumferential displacement (flow swirl) of the distorted region is assumed. When particle swirl is taken into account, however, there is a region of relatively low total temperature in the rear stages of the low total pressure region. This results in lower corrected flow and higher corrected speed in these stages relative to conditions that would normally be obtained with a uniform inlet and the same inlet values of corrected flow and speed. There is thus a tendency to increase incidence in the rear stages which effects a rematch of the front-to-rear loading distribution of the compressor stages. A similar rematch in the reverse direction occurs in the undistorted region of the compressor. The net effect of the rematch is to reduce the circumferential variation in velocity at the front and increase the velocity variation at the rear of the compressor relative to that calculated from parallel compressor theory. The consequences of particle swirl with respect to the distorted stall line are therefore dependent on the axial location of the limiting stage.

REFERENCES

1. "Compressor-Diffuser Interaction with Circumferential Flow Distortion", by E. Greitzer and H. Griswold, Project SQUID Workshop Proceedings, July, 1974.

2. "Attenuation of Circumferential Inlet Distortion in Multistage Compressors", by G. Plourde and A. Stenning, AIAA Paper (67-415, August, 1967).

3. "Hydrodynamics" by Sir Horace Lamb, Dover Publications, 1945, (pp. 51, 71).

4. "A Study of Perforation Configurations for Supersonic Diffusers", G. McLafferty, UARL Report R-53372-7, December, 1950.

LIST OF SYMBOLS

A	Area
a	Sonic Velocity
b	Chord Length
Cp	Specific Heat at Constant Pressure
h	Enthalpy
N1	Low Rotor Speed
N2	High Rotor Speed
p, P	Pressure
s	Entropy
T	Temperature
t	Time
u, U	Velocity
α, β	Air Angle
δ	Perturbation Quantity
θ_{T2}	Inlet Corrected Temperature
θ_{T3}	HPC Inlet Corrected Temperature
ρ	Density
τ	Empirical Time Constant
ω	Circular Frequency

SUBSCRIPTS

o, T	Total Conditions
INLET, I	Inlet
2	Exit
$-\infty$	Upstream Infinity
x	Axial Direction
Q.S.	Quasi-steady Value

SUPERSCRIPTS

$-$	Average
$'$	Perturbation Quantity

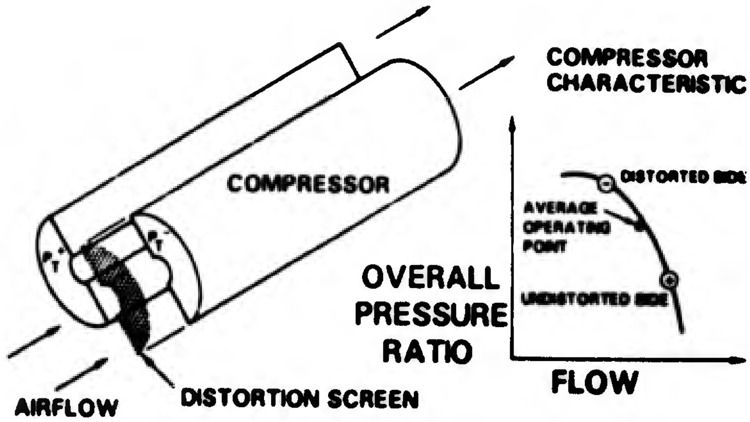

Figure A-1 Parallel Compressor Distortion Analysis

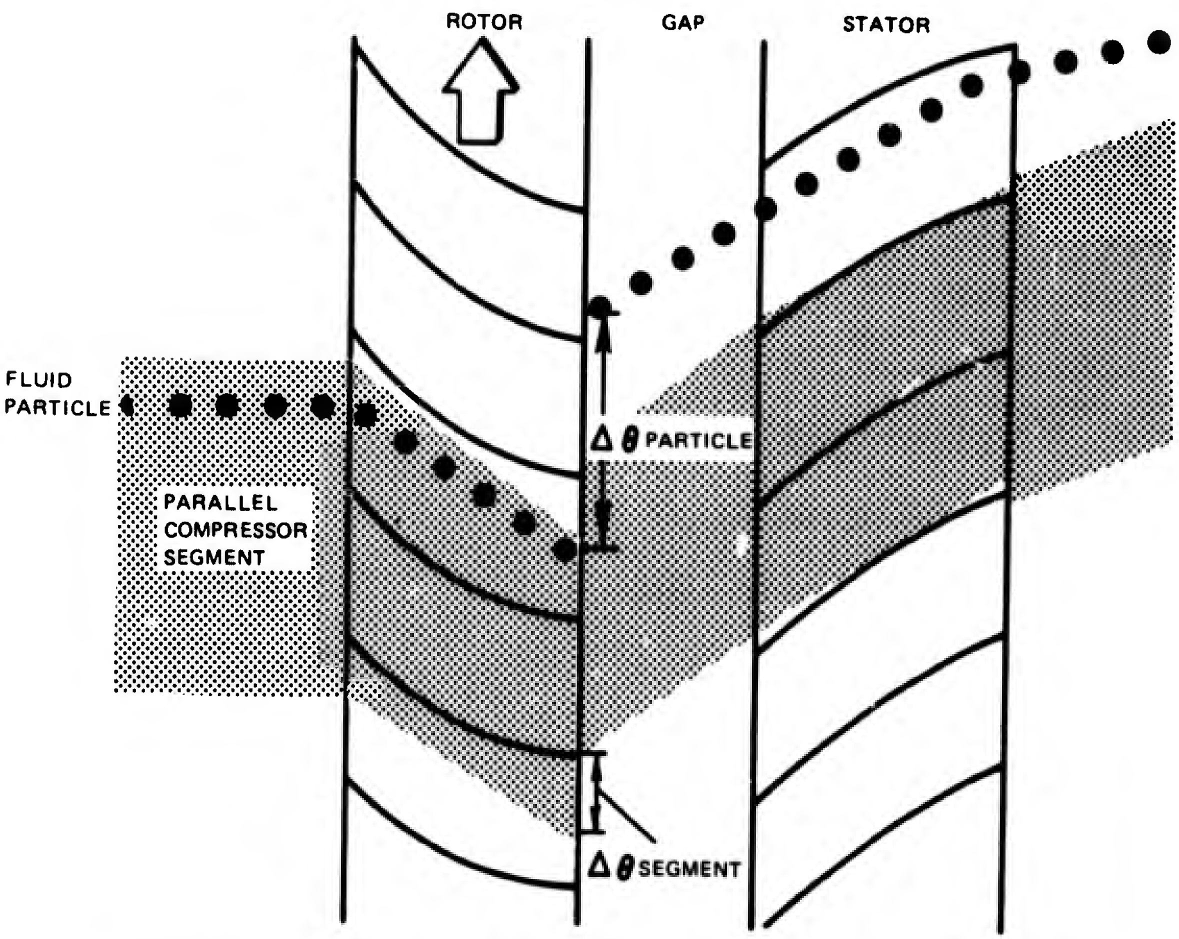

Figure A-2 Segment (Flow) and Particle Swirl Through A Compressor

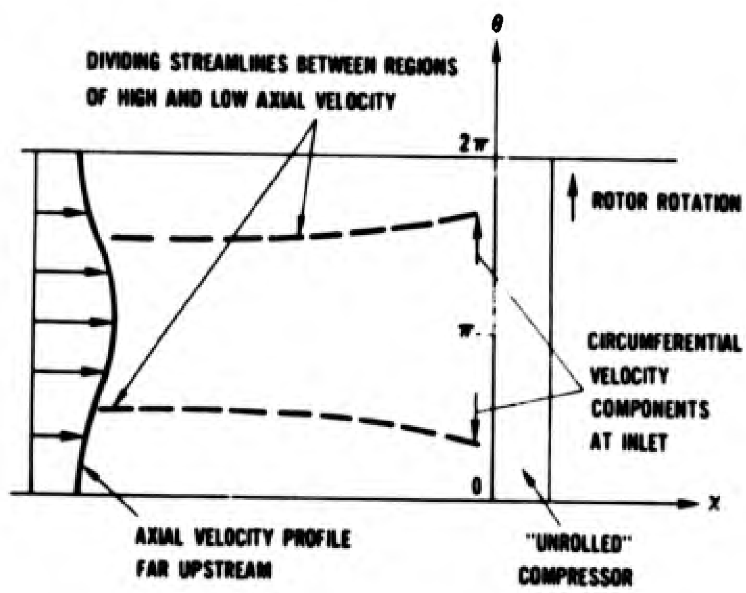

Figure A-3 Asymmetric Flowfield Upstream of Compressor

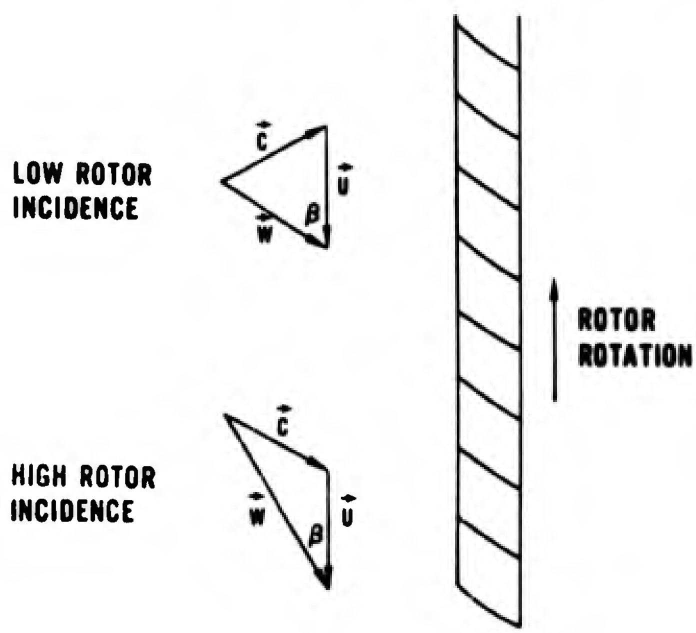

Figure A-4 Effect of Upstream Circumferencial Velocity on Rotor Incidence

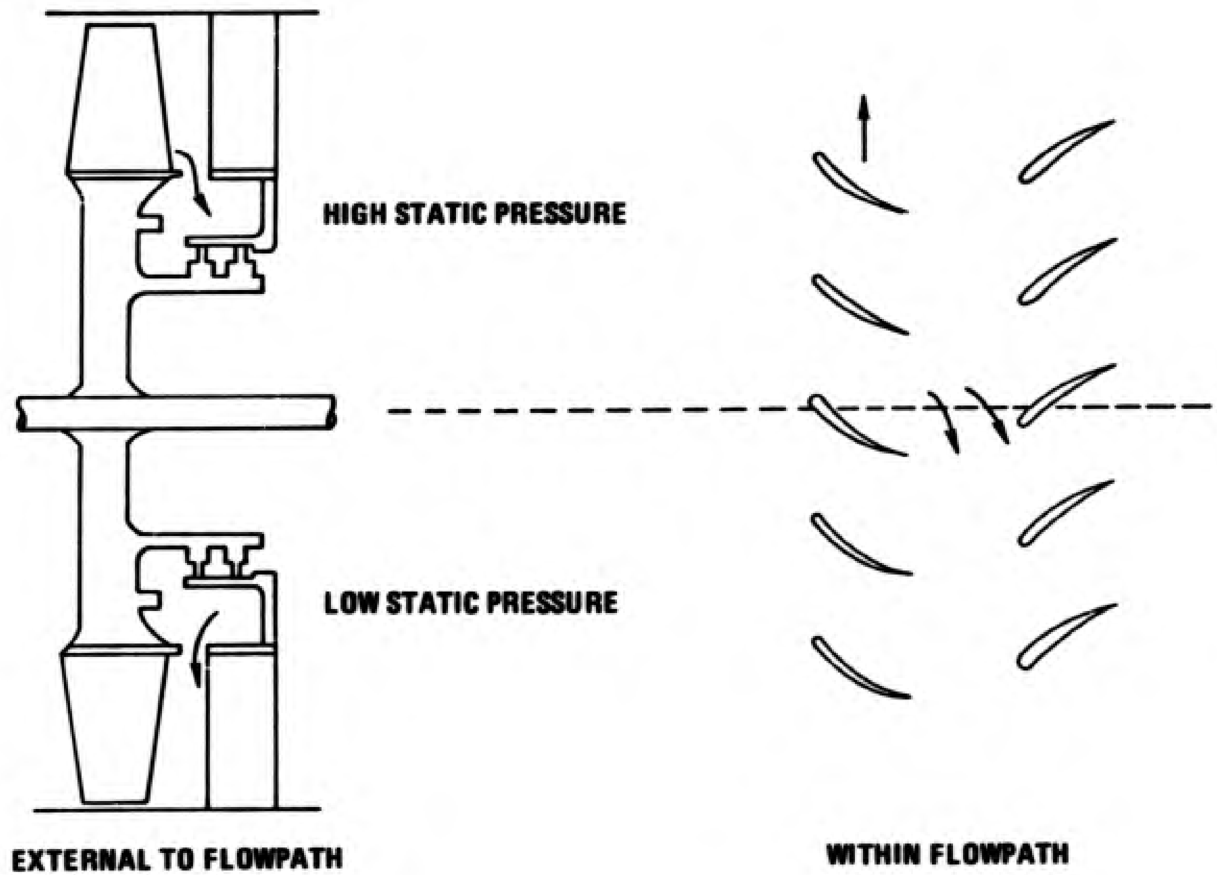

Figure A-5 Circumferential Flow in a Compressor Subjected to Circumferential Inlet Distortion

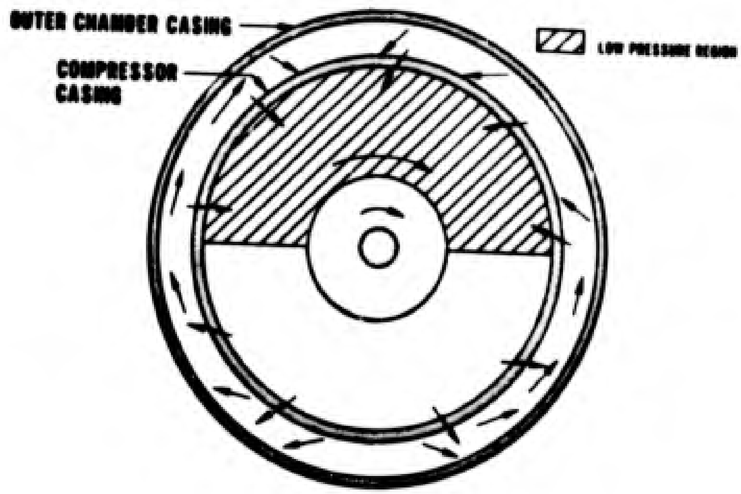

Figure A-6 Flow Redistribution Due to External Flow Chamber

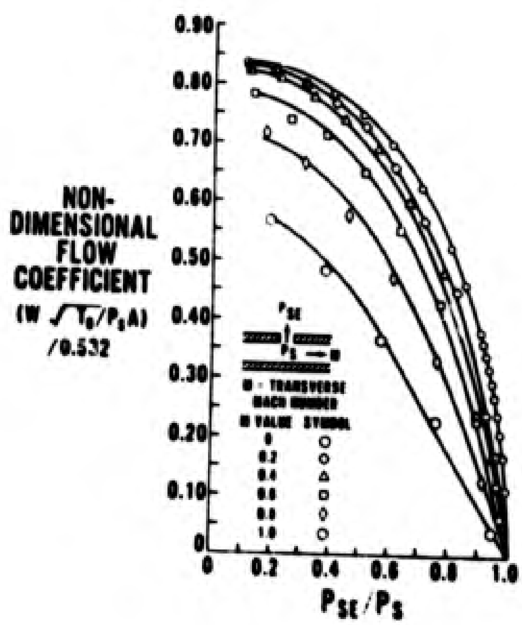

Figure A-7 Flow Coefficients for Passages From Flowpath to External Cavities

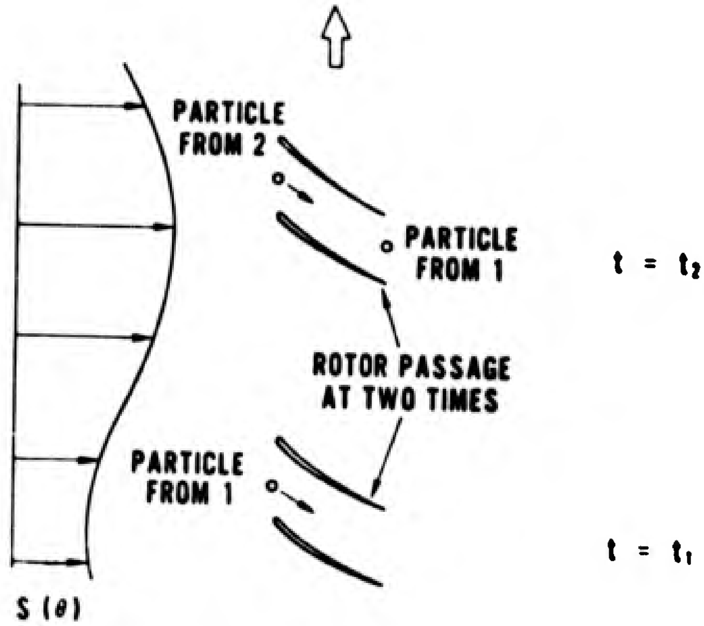

Figure A-8 Entropy Difference Due to Rotor Rotation

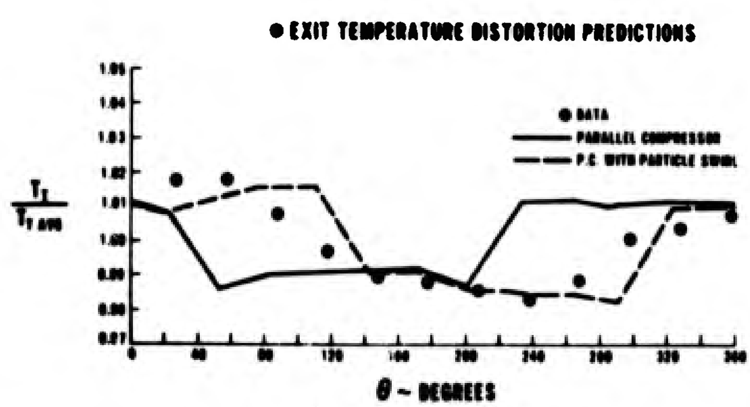

Figure A-9 Particle Swirl Effect

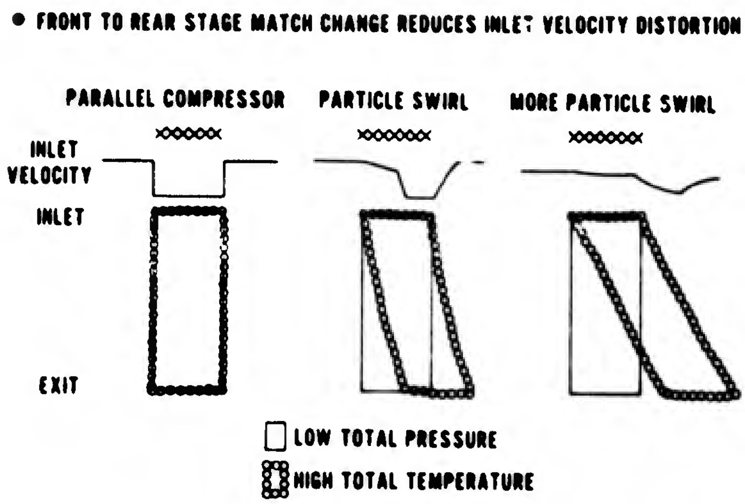

Figure A-10 Particle Swirl Effect

APPENDIX B

MOC Model

The problem addressed by this model is the solution of the time unsteady equations of motion for planar flow disturbances in a compression system. These flow disturbances take the form of inlet total pressure and temperature as well as exit static pressure. The method of characteristics has been chosen as the calculation procedure because it embodies the physical mechanisms of pressure wave and fluid particle propagation through the compressor. This insures the accurate phasing of events as the flow field changes with time. Furthermore, an algorithm has been constructed which enables the compressor blade performance maps to be used over a portion of a rotor or a stator. Previously, these maps have been used over the entire rotor/stator in a single step, thus giving erroneous propagation of waves through the rotor/stator. This algorithm provides a more realistic propagation of waves through compressors than has previously been possible with nonsteady compressor flow models.

Equations of Motion

The equations of motion solved are those for the one-dimensional conservation of mass, momentum and energy. These are expressed by the following relations in differential form:

Conservation of Mass

$$\frac{\partial (\rho A)}{\partial t} + \frac{\partial (\rho U A)}{\partial x} = 0 \qquad (1)$$

Conservation of Momentum

$$\frac{\partial (\rho U A)}{\partial t} + \frac{\partial (\rho U^2 A)}{\partial x} + Ag \frac{\partial p}{\partial x} - g \frac{\partial \Gamma}{\partial x} = 0 \qquad (2)$$

Conservation of Energy

$$\frac{Ds}{Dt} - \frac{1}{T} \frac{DQ}{Dt} - \frac{DSc}{Dt} = 0 \qquad (3)$$

These relations compose a set of partial differential equations necessary to solve for the time unsteady flow through a compressor. They can, however, be expressed in terms of total time derivatives of properties along certain "characteristic" directions or paths. These paths are those describing the motion of forward and rearward traveling pressure waves and fluid particles. They are expressed by the following:

Preceding page blank

Forward Traveling Pressure Wave

$$\frac{dx}{dt} = u + a \tag{4}$$

Rearward Traveling Pressure Wave

$$\frac{dx}{dt} = u - a \tag{5}$$

Fluid Particle

$$\frac{dx}{dt} = u \tag{6}$$

Let us now define $\delta_{\pm}/\delta t$ to denote differentiation with respect to time along the first two of these characteristics:

$$\frac{\delta_+}{\delta t} = \frac{\partial}{\partial t} + (u + a)\frac{\partial}{\partial x}$$

$$\frac{\delta_-}{\delta t} = \frac{\partial}{\partial t} + (u - a)\frac{\partial}{\partial x}$$

with the differentiation along the particle path having its usual definition,

$$\frac{D}{Dt} = \frac{\partial}{\partial t} + u\frac{\partial}{\partial x}$$

It is now possible to expand the equations of motion in terms of derivatives along the characteristic directions:

Along $\frac{dx}{dt} = u + a$

$$\frac{\gamma g R}{\gamma - 1}\frac{\delta_+ T}{\delta t} + a\frac{\delta_+ U}{\delta t} - JgT\frac{\delta_+ S}{\delta t} = -\frac{ua^2}{A}\frac{dA}{dx} +$$

$$\frac{ga}{\rho A}\frac{d\Gamma}{dx} + \frac{Ja^2}{R}\frac{(\gamma - 1)}{\gamma}\frac{DS}{Dt} \tag{7}$$

Along $\frac{dx}{dt} = u - a$

$$\frac{\gamma g R}{\gamma - 1} \frac{\delta_{-} T}{\delta t} - a \frac{\delta_{-} u}{\delta t} - JgT \frac{\delta_{-} S}{\delta t} = - \frac{ua^2}{A} \frac{dA}{dx}$$

$$- \frac{ga}{\rho A} \frac{d\Gamma}{dx} + \frac{Ja^2}{R} \frac{(\gamma - 1)}{\gamma} \frac{DS}{Dt} \qquad (8)$$

Along $\frac{dx}{dt} = u$

$$\frac{Ds}{Dt} = \frac{1}{T} \frac{DQ}{Dt} + \frac{DSc}{Dt} \qquad (9)$$

Once the flow field properties have been defined at some initial time t_o, it is possible to evaluate them at a later time $t_o + \Delta t$ through the numerical integration of equations 7-9 along their respective characteristic directions. See Figure B-1.

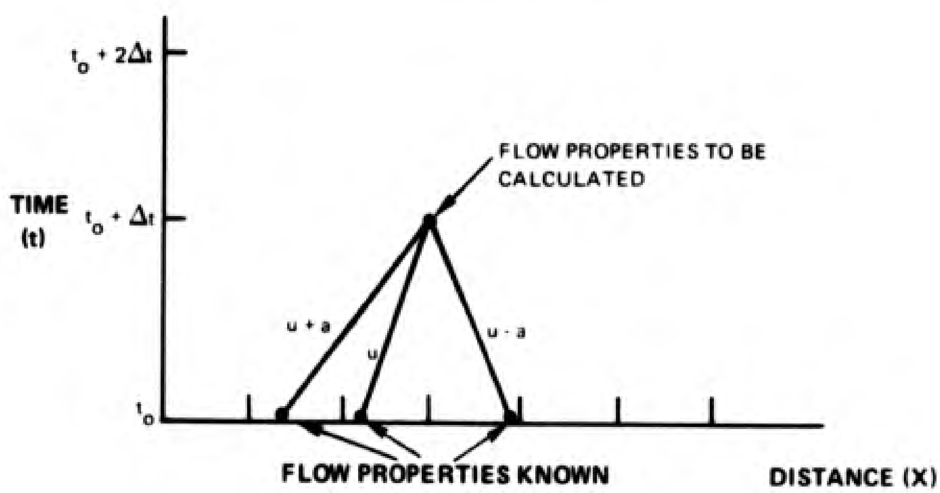

METHOD OF CHARACTERISTICS CALCULATION PROCEDURE

Figure B-1 Method of Characteristics Calculation Procedure

A simultaneous iterative solution of the equations is required because the derivatives of the various flow properties are differenced over the time interval from t_o to $t_o + \Delta t$. After the complete flow field solution has been obtained, at $t_o + \Delta t$, the process is repeated for additional time intervals until the desired transient flow process has been completed.

Algorithm for Blades

Since the axial locations at which the characteristics intersect the horizontal axis (Figure B-1) at time t_0 are not necessarily at the leading or trailing edge of a blade row, it is necessary to represent fluid properties at these locations in some manner. The simplest approximation that can be made is a linear variation of a sufficient number of fluid properties to define the internal flow field. Flow velocity, static temperature and static pressure are assumed to vary linearly across each blade row. The other necessary flow property, entropy, is defined from the pressure and temperature. This algorithm insures continuous flow field properties and provides an accurate calculation for disturbance propagation across rotors and stators.

Nomenclature

ρ	Density (lbm/ft^3)
A	Area (ft^2)
U	Velocity (ft/sec)
t	Time (sec)
x	distance (ft)
g	gravitational acceleration constant (32.2 $\frac{lbm\ ft}{lb_f\ sec^2}$)
p	pressure (lbf/ft^2)
Γ	blade force (lbf)
S	entropy (BTU/lbm °R)
T	temperature (°R)
Q	heat energy (BTU/lbm)
Sc	Entropy associated with compressor blades working on the fluid (BTU/lbm °R)
J	Joules constant (778. ft lbf/BTU)
R	gas constant (53.3 ft lbf/lbm °R)
γ	ratio of specific heats